

Application of Wavelets in Two Dimensional Gel Electrophoresis Image Analysis

Project Report

Wavelet Course Project

submitted by
TEAM — 4[†]

Under the guidance of
Prof. Vikram Gadre



Indian Institute of Technology, Bombay
2012

Project Report Approval Sheet

This is to certify that the project report entitled

Application of Wavelets in Two Dimensional Gel Image Analysis

by
TEAM 4[†]

¹ Satyaprakash Parikh ² Bhushan N Kharbikar ³ V Rajiv Ram ⁴ Pinaki Chandra Dey
⁵ Sudipta Sadhu ⁶ Mohan Sai Koushik ⁷ Antony Rajan ⁸ Dessie Fentaw ⁹ Karan Rampal
¹⁰ Ajay Sisodiya ¹¹ Darshan Mandge ¹² Nikhil Prakash ¹³ Rahul Sharma ¹⁴ Abhijeet Alase
¹⁵ Surabhi Sachdev ¹⁶ Chaitali Joshi

is approved.

Prof. Vikram Gadre

CONTENTS

1 Introduction.....	4
2 Proteomics and Two Dimensional Electrophoresis	6
2.1 Proteomics.....	7
2.2 Proteome Analysis.....	8
2.3 Two Dimensional Gel Electrophoresis.....	11
2.4 Generalized laboratory process.....	12
3 Image Analysis of 2D gel using wavelets	14
3.1 Image processing work flow.....	14
3.2 Comparative study of wavelets for its application in IA	15
3.3 Image De-Noising, using statistical model.....	21
3.4 Image De-Noising, non-parametric approach.....	27
3.5 Image Segmentation.....	36
4 Summary, Discussion and Conclusion.....	47
4.1 Comparative study of wavelets	47
4.2 Image De-Noising, using statistical model.....	48
4.3 Image De-Noising, non-parametric approach.....	49
4.4 Image Segmentation.....	49
5 References.....	50

CHAPTER 1

INTRODUCTION

The field of proteomics or proteome analysis has become an increasingly important part of the life sciences, especially after the completion of sequencing the human genome. Proteome analysis is the science of separation, identification, and quantitation of proteins from biological samples with the purpose of revealing the function of living cells. Applications range from prognosis of virtually all types of cancer over drug development to monitoring of environmental pollution.

Currently, the leading technique for protein separation is two-dimensional gel electrophoresis (2DGE), resulting in grey level images showing the separated proteins as dark spots on a bright background (see Fig. 1.1). Such an image can represent thousands of proteins.

In order to identify the protein *diversity* and to quantitate the protein *amount* in a biological sample, pattern analysis and recognition can be of help. It also seems natural to apply pattern analysis in the task of comparing this information with similar information from other samples or a database. A small region of 150×150 pixels is shown in detail.

Pattern analysis methods are currently applied in order to automate and ease the task of analysing gel images and comparing images from different biological samples, but with the current methods this part of the process requires large amounts of human-assisted work and it can be identified as the major bottle-neck in the total process from biological sample to protein identification and quantitation.

The most important breakthrough in proteomics has been:

- Introduction of immobilised pH gradients (1988) and
- Introduction of mass spectrometry in the 1990's.

What would lead to an equal breakthrough would be improved pattern recognition methods for analysis of the gel images, reducing the large amount of resources spent on human-assisted analysis of the gels and open-source and freely distributable advance analysis tool with source code. In other words, there is a great need for effective, reliable, and objective methods to analyse the enormous amounts of data coming from the proteomics research.

The pattern analysis of the 2DGE data is traditionally divided into two parts, namely the segmentation of the 2DGE images into what is protein spots and what are background, and the process of matching protein spot patterns across two or more gels. Correct segmentation results in quantitation of the spots that reflects accurately the amount of protein present. The matching enables to detect changes in protein expressions across samples, or even to identify new proteins.

This report provides study and analysis, with the main focus on application of wavelets to 2D-gel image for comparative study of best applicable wavelet, de-noising of gel images through statistical modeling and non-parametric method, and protein spot segmentation.

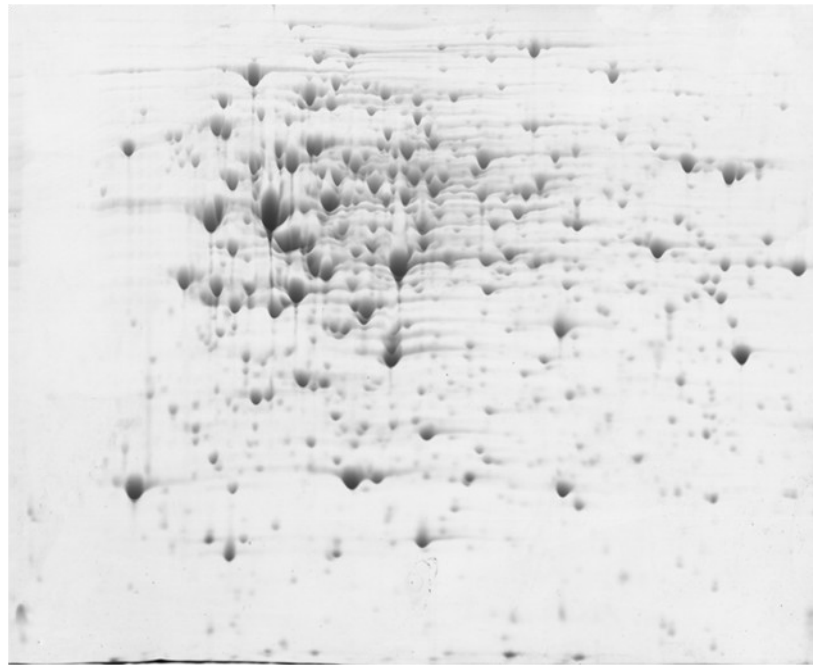


Figure 1.1 : Two dimensional gel electrophoresis gel image, Image courtesy : Proteomics Lab, IIT-B

CHAPTER 2

PROTEOMICS AND TWO DIMENSIONAL ELECTROPHORESIS

2.1 Proteomics

Proteomics is an increasingly important part of cell biology and the efforts to understand the basic principles of life – how the living cell works. This chapter will give some basic introductory knowledge to proteomics, the process of two-dimensional gel electrophoresis for protein separation, and the motivation for applying image analysis in the field of proteomics will be further explained.

In proteome analysis, gel electrophoresis is a technique to separate proteins in a biological sample on a gel. The resulting gel images are captured as a digital image of the gel. This image is then analysed in order to quantitate the relative amount of each of the proteins in the sample in question or to compare the sample with other samples or a database. The task of analysing the images can be tedious and is subjective (dependent on the human operator) if performed manually.

The use of digital image analysis in the field of proteomics is primarily motivated by the need to improve speed and consistency in the analysis of two-dimensional electrophoresis gel (2DGE) images.

The most important issues and challenges related to digital image analysis of the gel images will be described, namely the segmentation of the images and the matching of corresponding protein spots.

Knowledge of the basic principles in proteome analysis and gel electrophoresis provides a good background to understand the issues related to the image analysis part of the process – the main focus of this report.

2.2 Proteome analysis

A short definition of proteome analysis is: identification, separation and quantitation of proteins. The first publication of the word proteome was in 1995 by Wasinger et al. [2], and Wilkins [3] defines the concept of proteome analysis:

Proteome Analysis: “*The analysis of the entire PROTein complement expressed by a genOME, or by a cell or tissue type*”.

In other words, the proteome is the complete set of proteins that is expressed, and modified following expression, by the genome at a given time point and under given conditions in the cell.

The proteome provides us with much more information about the working of the living cell than the genome does. The genome is static and essentially identical in all somatic cells of an organism [4], where the proteome is constantly changing, reflecting the cell environment and also responding to both internal and external stimuli. The complete sequencing of the genome is not able to tell much about the function of the cell but analysis of the proteome is.

The techniques focused on here are two-dimensional gel electrophoresis (2DGE) combined with mass spectrometry (MS) and a general methods description for 2DGE and MS is given in Fey et al. [5]. A general introduction to the science of proteomics can be found in [6].

In the past years the extensive DNA sequencing efforts have provided hundreds of thousands of open reading frames in international databases. Unfortunately, a large proportion of this information has no or very little homology to any known protein. As one goes up the evolutionary tree this proportion increases (see Fig. 2.1) and even for one of the most extensively studied organisms, the relatively simple humble baker’s yeast (*Saccharomyces cerevisiae*) 63% of the genes have either no or only limited homology to known proteins.

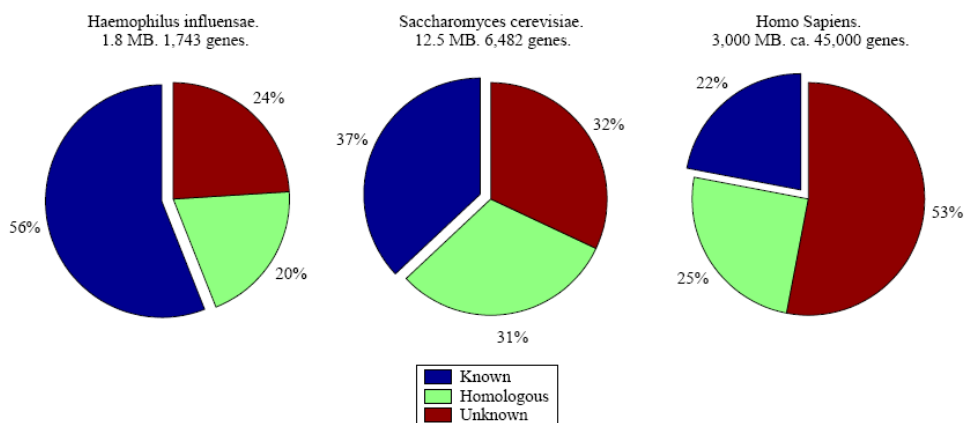


Figure 2.1: Division of sequenced genes into known, homologous and unknown categories for three different organisms. Data from CPA.

Furthermore, even when the open reading frame has some homology and the protein's function can be guessed at, many questions remain unanswered. These are questions as: Under what condition is the protein expressed? Where is it expressed in the organism? Where in the cell is it used? How is its expression regulated? Is the protein's expression affected in diseases (e.g. cancer, cardiovascular, auto-immunity or inflammatory diseases)?

To find answers to these questions is basically the motivation for studying the function of the gene products, namely the function of the proteins. By analyzing expression patterns of the proteins under different conditions the function of particular genes can be determined and some of the questions posed above may be answered.

Biological applications

Proteome analysis has a number of biological applications, examples include

- Understanding of the basic principles of life,
- Relating the genome and the environment to the organism's phenotype,
- Drug development/evaluation (including toxicology and mechanism of action),
- Disease prognosis, diagnosis, screening, monitoring of e.g., diabetes, all types of cancer, cardiovascular, and many more
- Identification of new drug or vaccine targets,
- Improvement of food quality,
- Monitoring environmental pollution, and
- Prevention of microorganism/parasite infections.

For instance in drug development, pharmaceutical companies spend large amounts of resources on studying the drug effect in animal experiments. Some of these effects can be assessed by measuring changes in protein levels across different tissue samples.

2.3 Two-dimensional gel electrophoresis

Two-dimensional gel electrophoresis (2DGE) enables separation of mixtures of proteins due to differences in their isoelectric points (pI), in the first dimension, and subsequently by their molecular weight (MWt) in the second dimension as sketched in Fig. 2.2.

Other techniques for protein separation exist, but currently 2DGE provides the highest resolution allowing thousands of proteins to be separated. For a review of the latest developments in the proteomics field, please refer to Fey and Mose Larsen [4], where 2DGE and some of the candidate technologies to potentially replace 2DGE are presented along with their advantages and drawbacks.

The great advantage of this technique is that it enables, from very small amounts of material, the investigation of the protein expression for thousands of proteins simultaneously. After protein separation an image of the protein spot pattern is captured. Proper finding and quantitation of the protein spots in the images and subsequent correct matching of the protein spot patterns allows not only for the comparison of two or more samples but furthermore makes the creation of an image database possible.

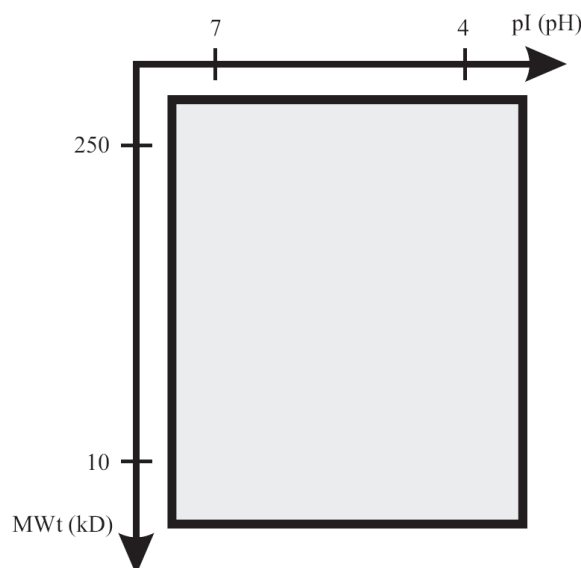


Figure 2.2: Schematic two-dimensional electrophoresis gel. Proteins are separated in two dimensions; horizontally by iso-electric point (pI) and vertically by molecular weight (MWt). No proteins shown. The pI and MWt ranges are example values.

The changes in protein expression, for example in the development of cancer are subtle: a change in the expression level of a protein of a factor 10 is rare, and a factor 5 is uncommon. Furthermore, few proteins change: usually less than 200 proteins out of 15,000 would be expected to change by more than a factor 2.5. Multiple samples need to be analysed because of the natural variation, for example between individuals and therefore it is necessary to be able to rely on perfect matching of patterns of the new images.

Even though promising attempts have been made to make the technique as reproducible as possible there are still differences in protein spot patterns from run to run. Also due to improvements in the composition of the chemicals used to extract as many proteins as possible the patterns become so dense (crowded) that locating the individual protein spots is a non-trivial task.

2.4 Generalized laboratory process

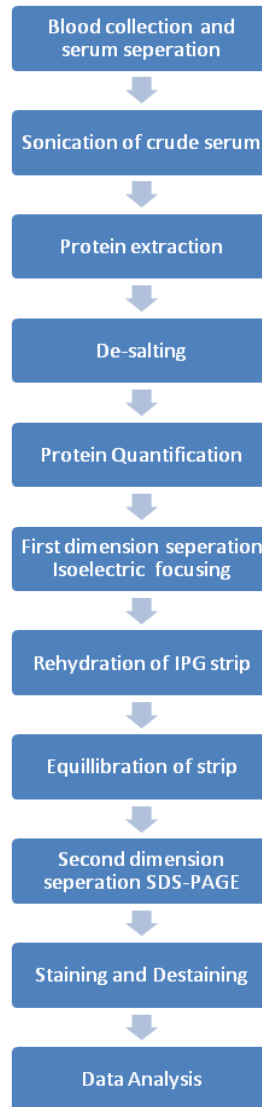


Figure 2.3: Process flow depicted for human serum proteome analysis by 2DGE. Data courtesy Proteomics Laboratory, IIT-Bombay

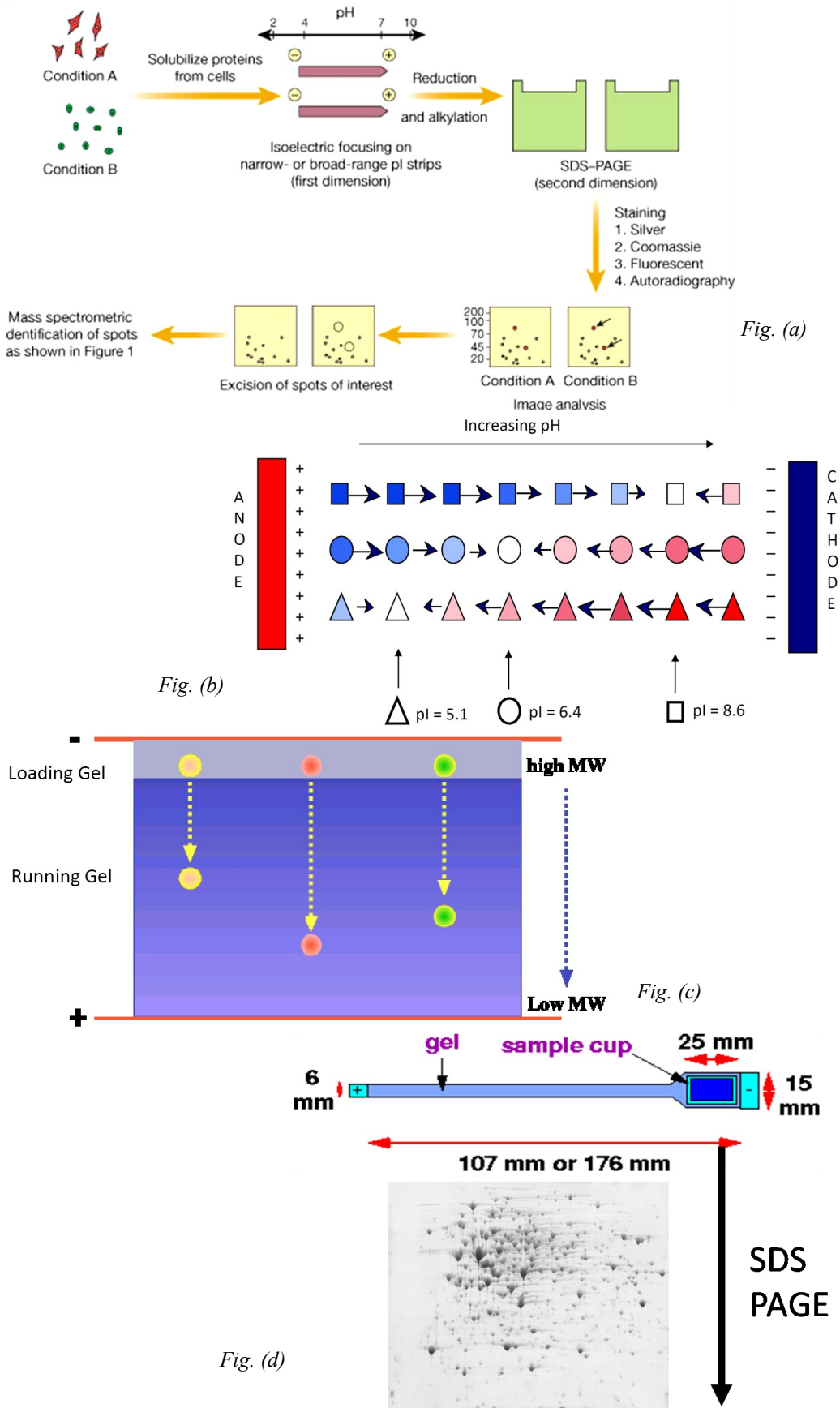


Figure 2.4: Diagram of the 2DGE process. (a), (b) & (c) By courtesy of CPA (Centre for Protein Analysis), (d) By courtesy of Proteomics Lab, Indian Institute of Technology, Bombay.

CHAPTER 3

IMAGE ANALYSIS of 2D GEL USING WAVELETS

3.1 Image processing work flow

In general, the traditional image processing pipeline for 2-DE includes [5]:

- Pre-processing of the gel images.
- Spot segmentation, modeling and expression quantification.
- Image registration to correct for geometric & intensity deformation and for image matching and spot comparison to derive statistical vectors for identification of differential expression of proteins.
- Interpretation, either by manual visualization or with data mining.
- Creation of federated 2-DE databases.

*There are few most fundamental operations while processing 2DE image mainly viz., **Image de-noising**, **Image Segmentation** and **Spot matching report** will now focus on detailing the different operations in Image Analysis with help of Wavelets.*

2D- Discrete Wavelet Transform

For images, there exist an algorithm similar to the one-dimensional case for two-dimensional wavelets and scaling functions obtained from one-dimensional ones by tensorial product.

This kind of two-dimensional DWT leads to a decomposition of approximation coefficients at level j in four components: the approximation at level $j + 1$, and the details in three orientations (horizontal, vertical, and diagonal).

The following chart describes the basic decomposition steps for images:

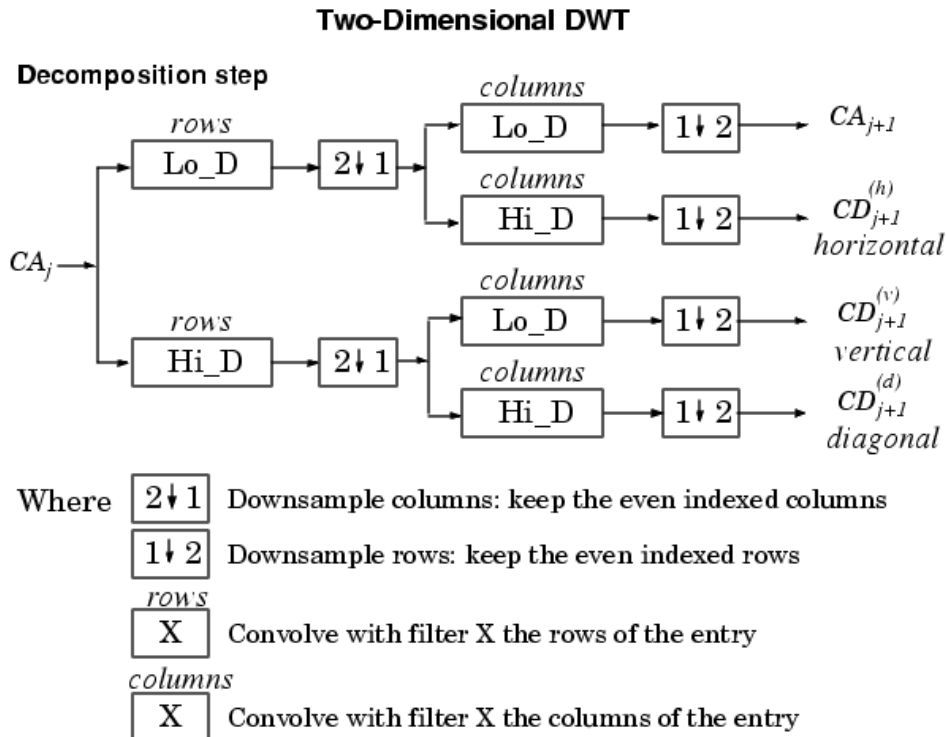


Fig 3.1 Describing how a 2d DWT works.

3.2 Comparative study of wavelets for its application in IA

Fewer studies have been performed on this line and fewer literature regarding comparison of wavelets for applications in proteomics is available, perhaps because the field is new and investigations in this direction have not started.

As can be seen in the denoising section of this report, wavelet denoising is a widely accepted method for denoising of images. This technique has also been used in denoising proteomic 2D gel images for protein spot identification purpose. Wavelets have also been used in statistical modeling for denoising, modeling

of spots segmentation. However, after going through some of the available literature, we felt the need of comparative study of wavelets for above mentioned applications.

The general approach is to determine parameters for each application (e.g. denoising) which can quantify the performance of each wavelet for that particular application. Then using those parameters, the performance of various wavelets of differing orders for that application on a large number of images has been compared to find out the wavelet which gives the best results for maximum number of images.

We chose two application for our study

1. Denoising
2. Spot characterization

3.2.1 Comparative Study for Denoising

- MATLAB generated noise (Gaussian and Salt Pepper) is superimposed on original image.
- The original image is decomposed into sub-bands by wavelet transform using various wavelets.
- On sub-bands of each transformed image, thresholding is performed using various methods like Bayes Soft and Bayes Hard, Unisoft, Uni-hard.

The image is reconstructed using backward wavelet transform.

To compare the level of denoising achieved using each wavelet, the parameter we have chosen is PSNR (Peak Signal to Noise Ratio) of denoised image with respect to original image. The description of denoising methods and PSNR parameter can be found in Denoising section.

The results obtained on many images using various wavelets are presented below.

3.2.2 Results

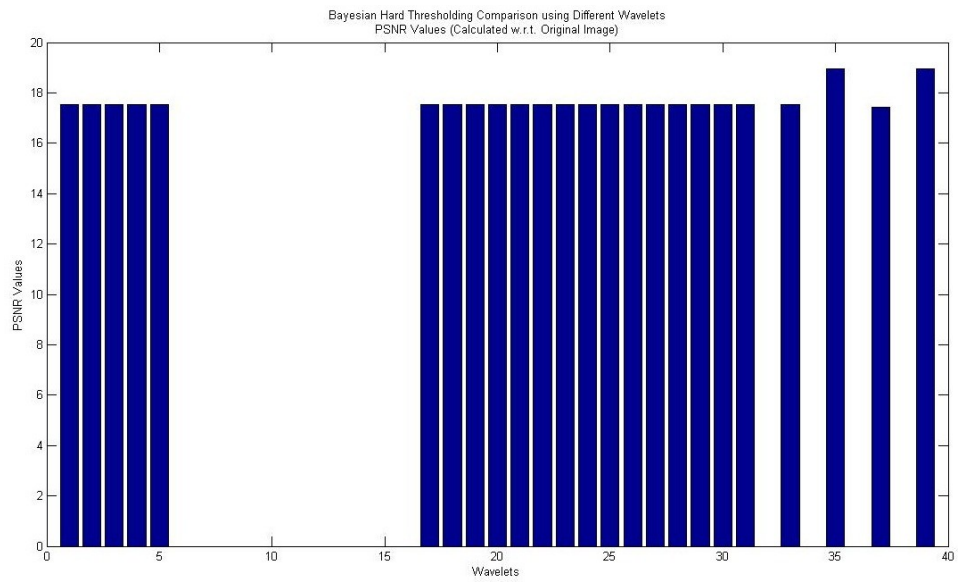


Fig (a)

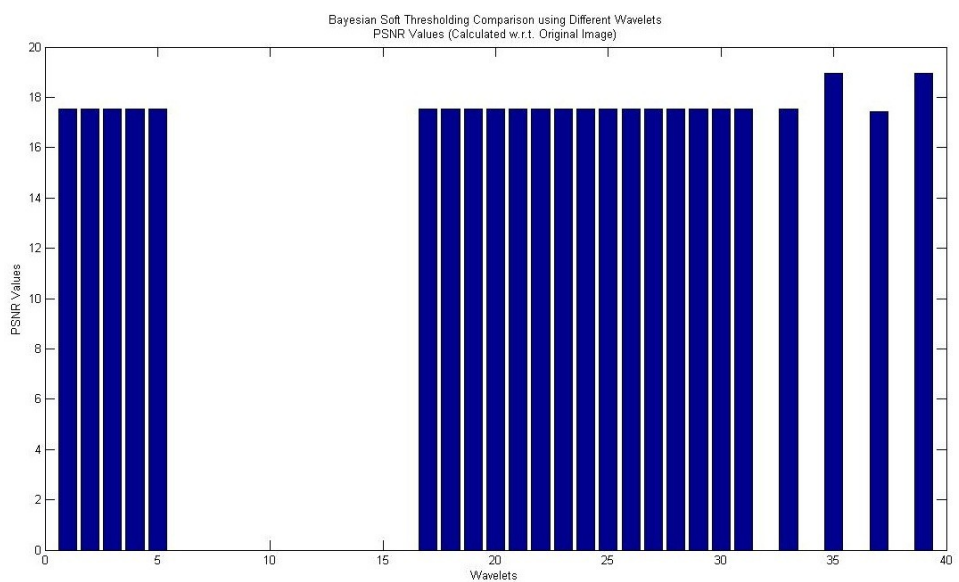


Fig (b)

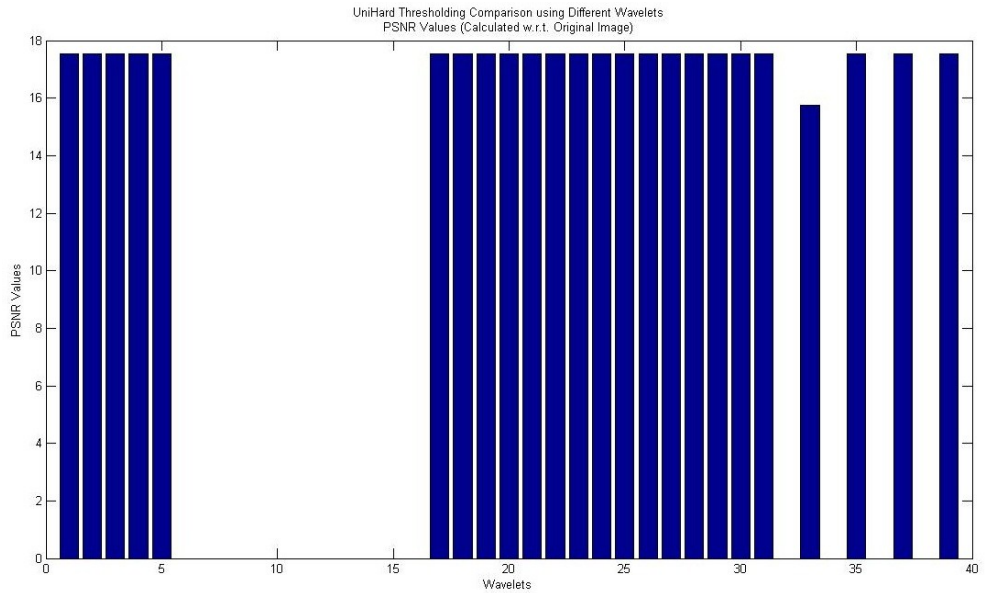


Fig (c)

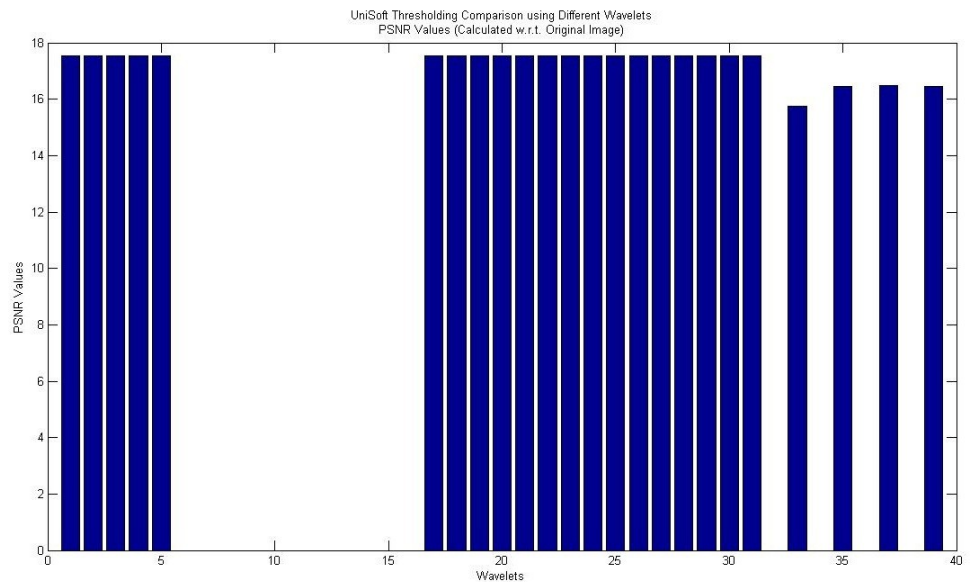


Fig (d)

Fig (a),(b),(c),(d) Wavelets used are
coif1,coif2,coif3,coif4,coif5,db1,db2,db3,db4,db5,db6,db7,db8,db9,db10,db11,db12, db13,db14,db15,haar,quincunx,undecimated-coif5,undecimated quincunx

3.2.3 Spot Characterization

As we had little idea about how to proceed in this part of the application, we started by analysing wavelet transforms of synthetic images. We also observed the transforms of real protein spots which we cropped from real images available on database. Before taking wavelet transforms, we denoised the images. By observation of many such images, we found that transforms of true protein spot images show an intensity pattern which is missing in fake spots. The transformed real spots in their detail band show a thick ring shaped pattern. The images in support of this observation are shown below.

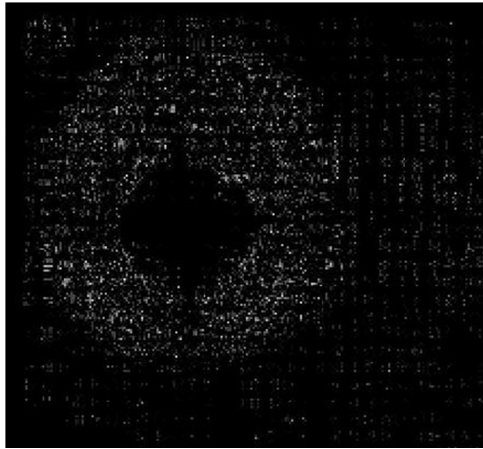


Fig 3.3 (a)

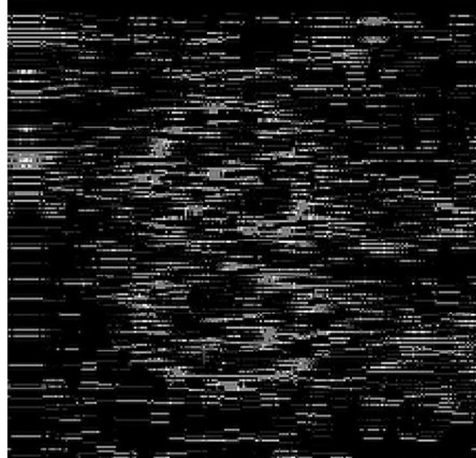


Fig 3.3 (b)

Figure 3.3: (a), (b) True and Fake protein spots respectively

The observed pattern in the detailed band for true spots is not absurd, and can be explained intuitively. As intensity distribution of true protein spots closely resembles that of a flat top gaussian, the intensity values of detailed band obtained in the plateau region (flat top) of true protein spot are very small, as compared to the values at the edges of the spot, where intensity of the spot image rises sharply. As opposed to true spots, in case of fake spots, the intensity of image varies almost linearly from the centre of the spot to its edge, and

and hence we do not observe the ring structure.

On the basis of this observation, we define a parameter “tubularity”. The value of this parameter is equal to the ratio of average intensity of detailed band in the region covered by complete outer ring in original image to the average intensity of detailed band in region covered by inside portion of the ring in original image. Since the average intensity in the region inside the ring is evidently small, we expect that this parameter will show larger values for true spot as compared to the fake spots. To identify the ring shaped regions in the detail band, we have looked at the real image and selected the regions which have intensity values less than corresponding thresholds set by us (say minimum intensity +20 for inner ring and maximum – 50 for outer ring) . (This intensity dependent selection of region at first appears not very good as it may capture other regions too. But our tests on various images prove that the parameter is quite robust to these additional regions being captured and is still enough to differentiate between true and fake spots)

We have implemented our code using various wavelets of different orders on a large number of true and fake spots. We are presenting some of the results here for comparison.

3.2.4 Results

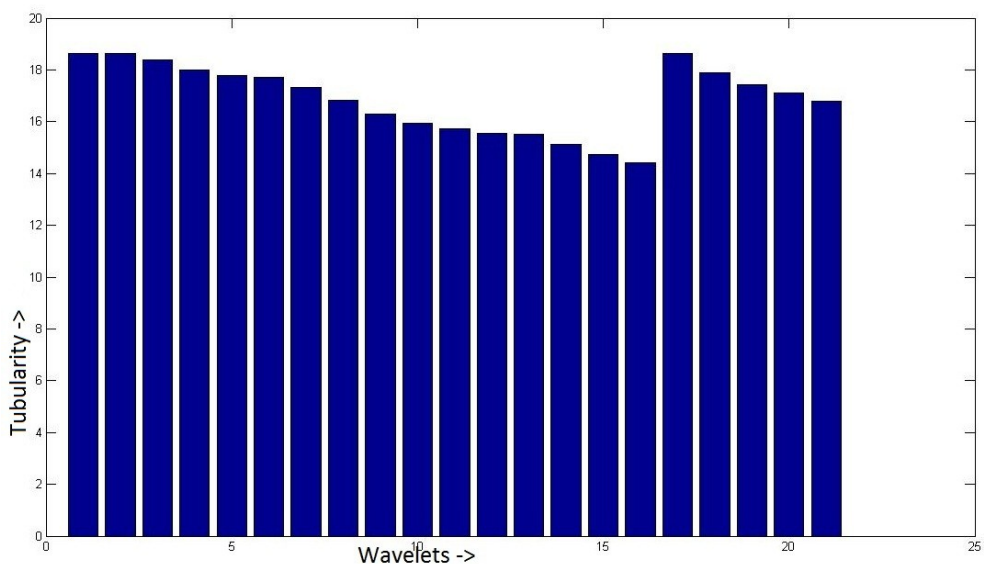


Fig 3.4(a) Tubularity plot for true spots

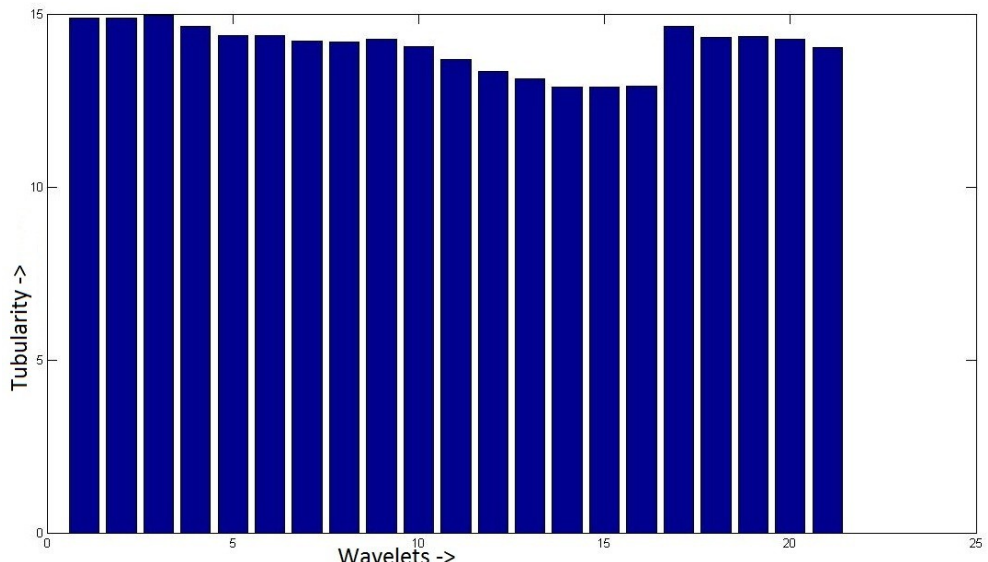


Fig 3.4 (b) Tubularity plot for Fake spot

3.3 Image De-Noising, using statistical model

Accurate image modeling, whether done explicitly or implicitly, is a critical component of many image processing tasks. In a simple yet effective statistical spatially-adaptive wavelet image model was demonstrated. In this work, we demonstrate a closely related model for image wavelet coefficients and apply it to denoising of 2D-gel images corrupted by Gaussian and Salt Pepper.

Demonstrated model significantly reduces the computational burden yet produces comparable results in terms of mean-squared error (MSE) and perceptual image quality. The key ingredient of algorithm is the use of simple but efficient spatial adaptation techniques. This paper does not attempt to investigate the theoretical properties of the proposed models and algorithms in general settings. Our primary goal is to demonstrate the importance of accurate modeling for image denoising problems in wavelet domain.

Algorithms is based on the Discrete Wavelet transform. The transform coefficients within subbands are modeled as independent identically distributed random variables with Generalized Gaussian distribution.

This model takes an approach which exploits the *local* structure of wavelet image coefficients. Also, uses linear Minimum Mean Squared Error(MMSE)-like estimation instead of coefficient thresholding.

3.3.1 Stochastic model for wavelet coefficients

Image wavelet coefficients are modeled as a realization of a doubly stochastic process. Specifically, the wavelet coefficients are assumed to be conditionally independent zero-mean Gaussian random variables, given their variances. These variances are modeled as identically distributed, highly correlated random variables. For estimation wavelet coefficients are approximated as local i.i.d.

Model features following characteristics as

- putting a stochastic prior on the local variances and
- model the wavelet coefficients as conditionally independent Gaussian random variables

It is assumed that image pixels are corrupted by AWGN and salt and pepper noise with known variance σ^2 . Let $X(k)$ represent the orthonormal wavelet coefficients of the “clean” image. The wavelet coefficients of the noisy image are given by $Y(k) = X(k) + n(k)$, where $n(k)$ is AWGN due to orthonormality of the chosen wavelet transform.

Denoising algorithm operates in two steps. Initially, perform an approximate MAP estimation of the variance $\sigma^2(k)$ for each coefficient, using the observed noisy data in a local neighborhood and a prior model for $\sigma^2(k)$. The estimate $\hat{\sigma}^2(k)$ is then substituted for $\sigma^2(k)$ in the expression for the MMSE estimator of $X(k)$.

3.3.2 Denoising algorithm

Given $\sigma^2(k)$, the wavelet coefficients $X(k)$ are independent Gaussian variables, so the MMSE estimator for $X(k)$ is given by

$$\hat{X}(k) = \frac{\sigma^2(k)}{\sigma^2(k) + \sigma_n^2} Y(k).$$

We emphasize that this assumes $\sigma^2(k)$ is deterministic and known. But in fact $\sigma^2(k)$ is not known, so we construct a linear MMSE-like estimator.

$$\hat{X}(k) = \frac{\hat{\sigma}^2(k)}{\hat{\sigma}^2(k) + \sigma_n^2} Y(k)$$

where $\hat{\sigma}^2(k)$ is an estimate for $\sigma^2(k)$.

Results indicate that the performance of the proposed approximate MMSE predictor is dependent, to some high extent, on the quality of the estimator $\hat{\sigma}^2(k)$.

3.3.3 Estimation of variance

The estimation of the variance field $\sigma^2(k)$ is the crux of the proposed denoising algorithm. For each data point $Y(k)$, an estimate of $\sigma^2(k)$ is formed based on a local neighborhood $N(k)$. We use a square window $N(k)$ centered at $Y(k)$. Assuming the correlation between variances of neighboring coefficients is high, we have $\sigma^2(j) = \sigma^2(k)$ for all j belongs to $N(k)$. Then we compute an approximate Maximum Likelihood (ML) estimator

$$\hat{\sigma}^2(k) = \arg \max_{\sigma^2 \geq 0} \prod_{j \in N(k)} P(Y(j) | \sigma^2) = \max \left(0, \frac{1}{M} \sum_{j \in N(k)} Y^2(j) - \sigma_n^2 \right)$$

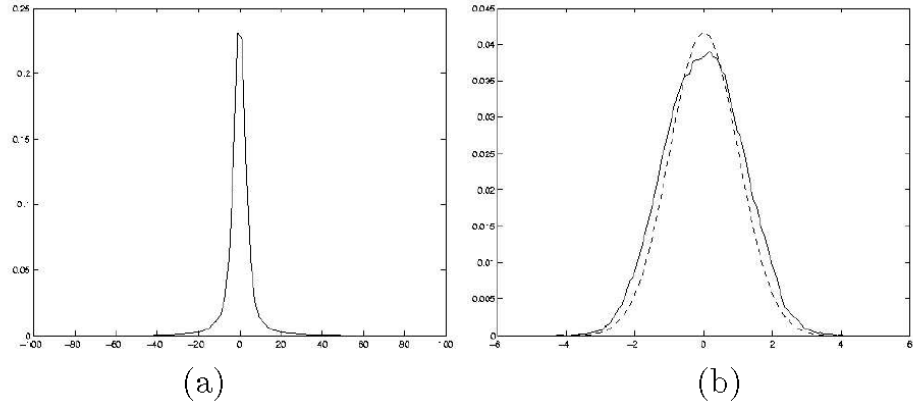


Figure 3.5 : (a) - Histogram of the high-band wavelet coefficients of Gel Image. (b) Solid line: histogram of the same coefficients scaled by estimated local standard deviations. Dashed line: unit-variance, zero-mean Gaussian p.d.f.

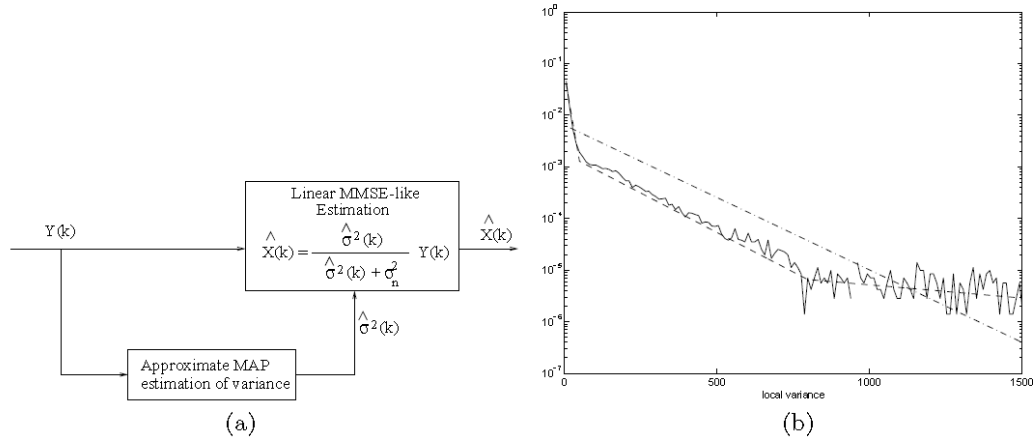


Figure 2: (a) Block-diagram of the denoising algorithm. For each observed noisy coefficient $Y(k)$ we form an approximate MAP estimate $\hat{\sigma}^2(k)$ of the variance of $X(k)$ based on a local neighborhood and on the prior $f\sigma$. The estimate $\hat{\sigma}^2(k)$ is then used for linear MMSE-like estimation of $X(k)$. (b) Histogram of the estimated local variance of the coefficients (solid line) in wavelet image subband approximated using a single exponential prior (dash-dotted line) and a mixture of exponentials that consists of three single exponentials in three non-overlapping regions (dashed line).

Now, assume a prior marginal distribution $f_\sigma(\sigma^2)$ for each $\sigma^2(k)$ is available. Then we obtain an approximate MAP estimator for $\sigma^2(k)$ as

$$\hat{\sigma}^2(k) = \arg \max_{\sigma^2 \geq 0} \left[\prod_{j \in \mathcal{N}(k)} P(Y(j)|\sigma^2) \right] f_\sigma(\sigma^2)$$

The exponential prior $f_\sigma(\sigma^2) = \lambda e^{-\lambda\sigma^2}$ is a reasonable candidate to fit the original histogram

The approximate MAP estimate for $\sigma^2(k)$ using an exponential prior is given by

$$\hat{\sigma}^2(k) = \max \left(0, \frac{M}{4\lambda} \left[-1 + \sqrt{1 + \frac{8\lambda}{M^2} \sum_{j \in \mathcal{N}(k)} Y^2(j)} \right] - \sigma_n^2 \right)$$

However it does not produce better image denoising results.

3.3.4 Results

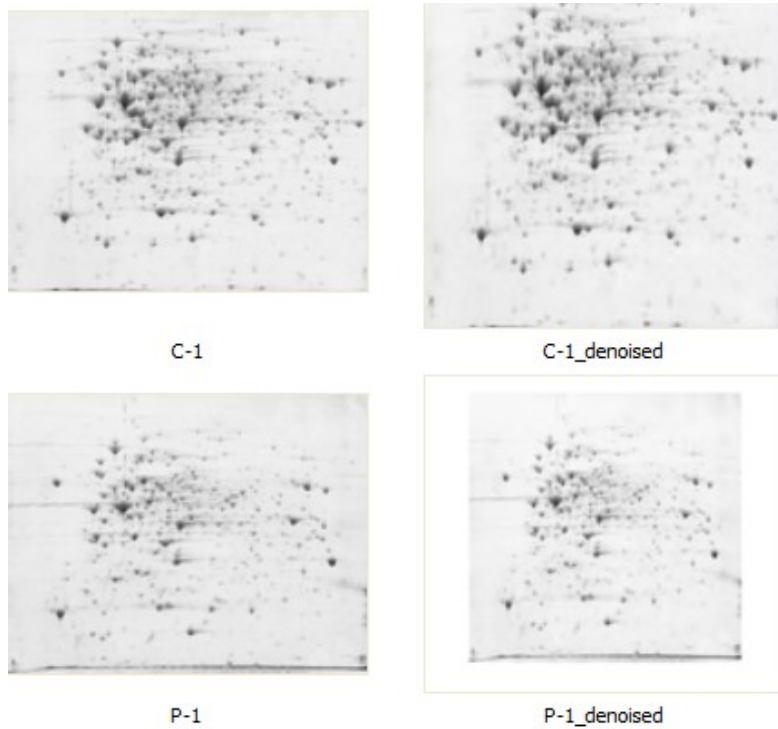


Fig (a)

Fig Noisy and Denoised gel images of healthy(c)and treated(p) gel
(a) using ML estimator

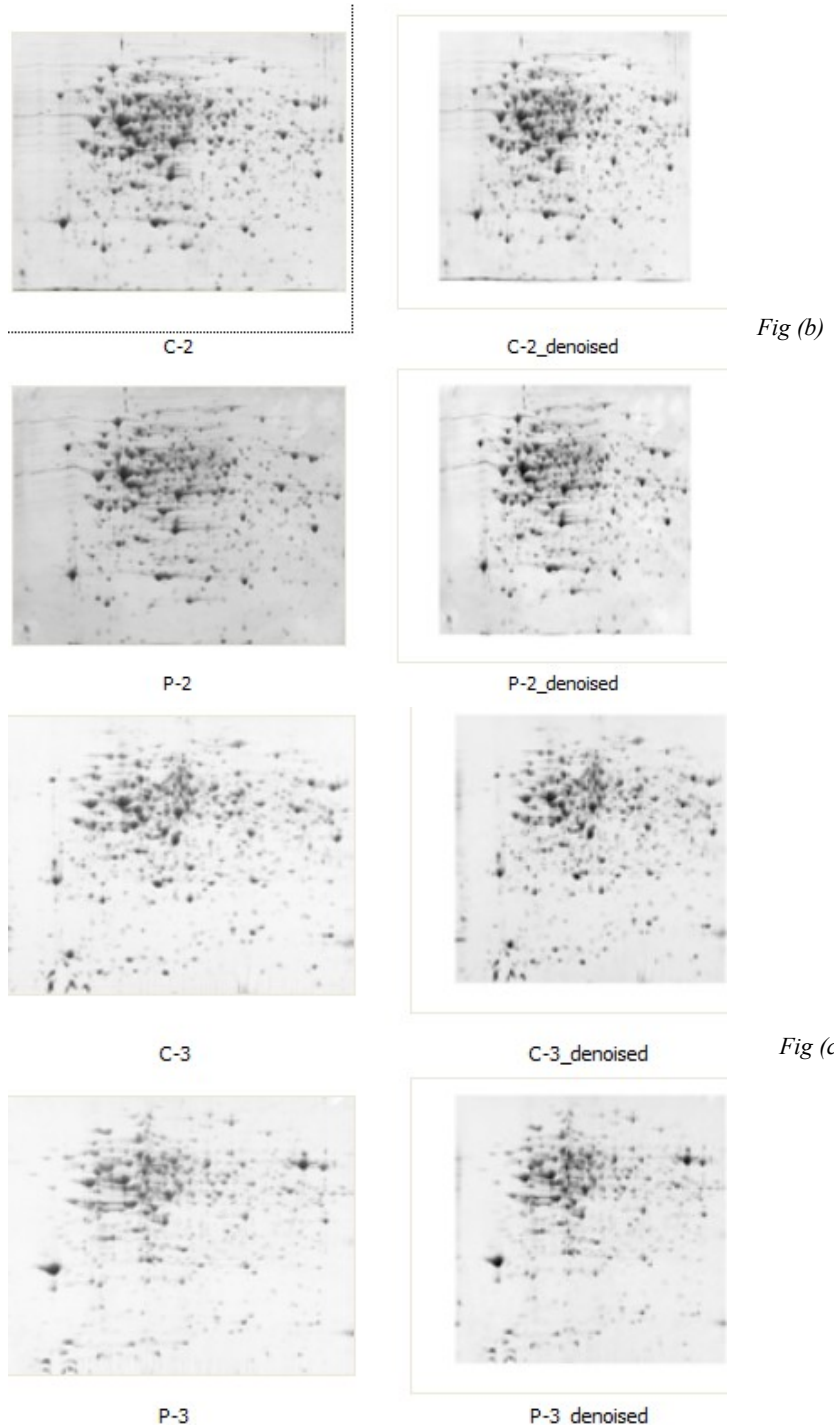


Fig Noisy and Denoised gel images of healthy(c)and treated(p) gel
(b)(c) using MAP estimator

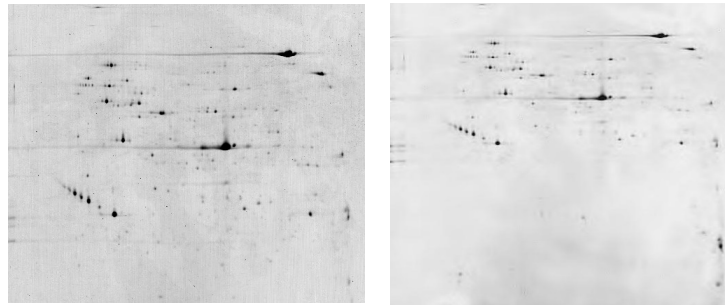


Fig (d)

Fig Noisy and Denoised gel images of healthy(c)and treated(p) gel using weiner's filtering

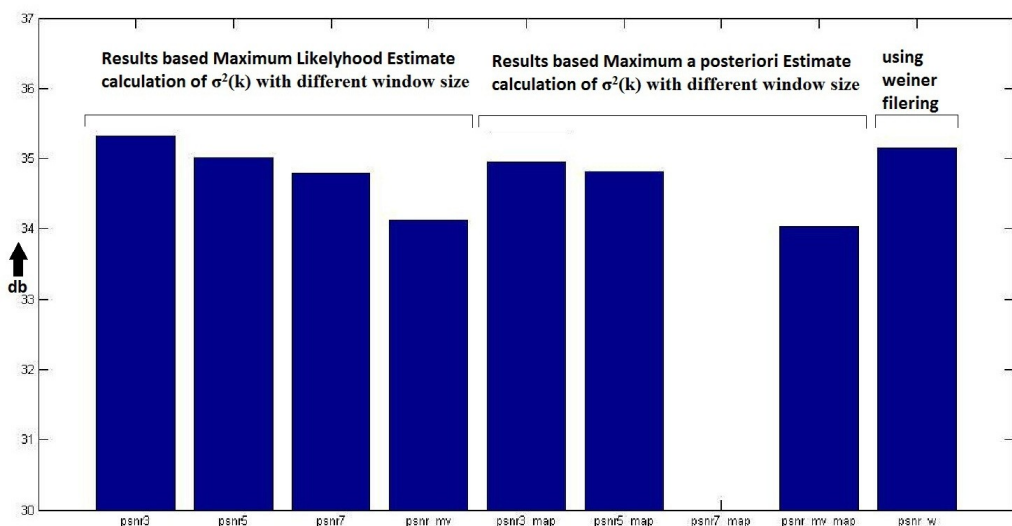


Fig Comparison of methods on basis of psnr of output

	Psnr3 ML	Psnr5 ML	Psnr7 ML	psnr_m v ML	psnr3_ MAP	psnr5_ MAP	psnr7_ MAP	psnr_mv_ MAP	psnr_w Weiner	
P1=	37.0813	36.5419	36.0658	35.0623	NaN	NaN	NaN	NaN	36.5339	
P2=	36.2291	35.7342	35.2604	34.2599	NaN	NaN	NaN	NaN	35.7567	
P3=	36.6723	36.1108	35.6693	34.6972	NaN	NaN	NaN	NaN	36.1398	
C1=	36.8988	36.3391	35.9172	34.9306	NaN	NaN	NaN	NaN	36.3547	
C2=	35.9271	35.37	34.9566	33.9822	35.2053	NaN	NaN	33.8591	35.3765	
C3=	36.2836	35.6651	35.2364	34.2502	35.3589	NaN	NaN	33.9956	35.6782	
Synthetic spot =	35.3167	35.0127	34.7827	34.1189	34.9416	34.814	7	NaN	34.0313	35.148

Table: Tabulation of all the psnr data recorded for the out images with obtained by employing different methods as described.

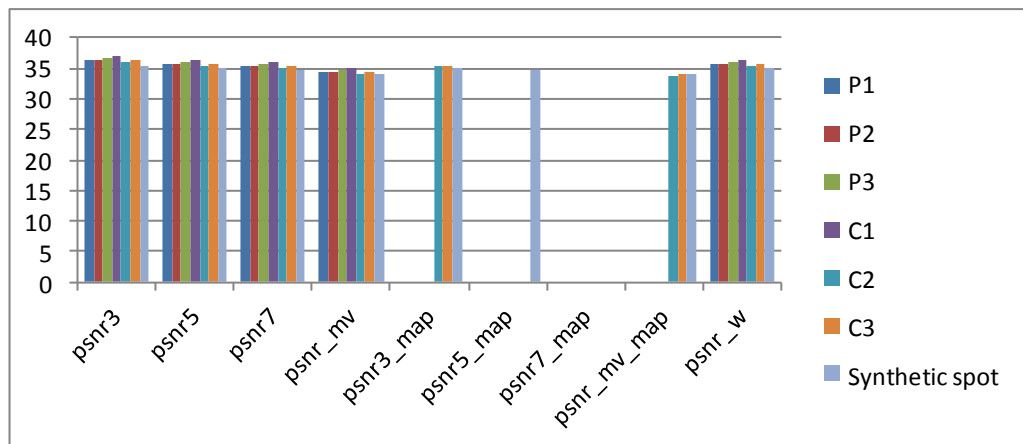


Fig: Histogram plot of Comparison of methods on basis of psnr of output images

3.4 Image De-Noising, non-parametric approach

Wavelet de-noising must not be confused with smoothing; smoothing only removes the high frequencies and retains the lower ones. Wavelet shrinkage is a non-linear process and is what distinguishes it from entire linear de-noising technique such as least squares.

A number of approaches have been developed which when used independently provide some degree of de-noising. One of the aims of this project was to come up with a protocol that could utilize the advantages of some of these approaches. In this regard the following approaches were selected and implemented:-

Discrete wavelet transform taken using:-

- a. Haar
- b. Daubechies (D4, D6, D8)
- c. Coiflet (C6)

Thresholding.

- Using both Soft and
- Hard Threshold.

Threshold selection will be done using the following approaches:-

- VisuShrink
- SureShrink
- BayesShrink

Application of Total Variation to further reduce noise and overcome the cons of Thresholding. Complex Wavelet Transform taken and steps 2 and 3 were again applied.

3.4.1 Motivation for Wavelet thresholding

The plot of wavelet coefficients is shown. This suggests that small coefficients are dominated by noise, while coefficients with a large absolute value carry more signal information than noise. Replacing noisy coefficients (small coefficients below a certain threshold value) by zero and an inverse wavelet transform may lead to a reconstruction that has lesser noise.

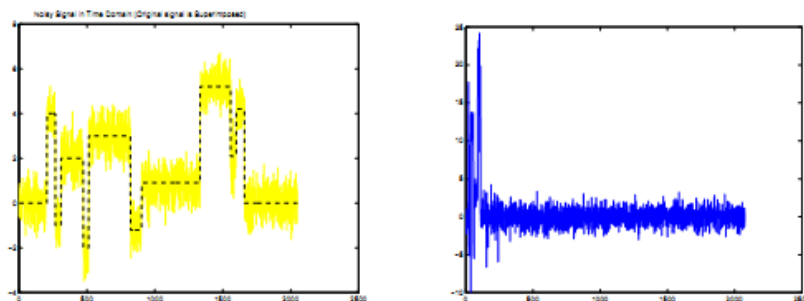


Fig: Noisy 1D signal and the plot of wavelet coefficients using Matlab.

As it turns out, this method is indeed effective and thresholding is a simple and efficient method for noise reduction. Further, inserting zeros creates more sparsity in the wavelet domain and here we see a link between wavelet de-noising and compression.

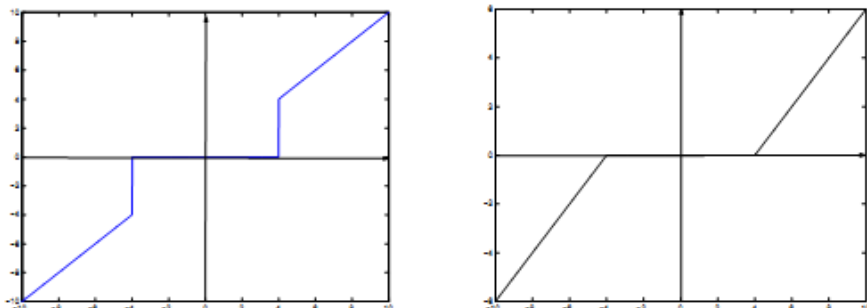


Fig: Hard thresholding and soft thresholding transfer functions generated using matlab

3.4.2 Hard and soft thresholding

Hard and soft thresholding with threshold λ , are defined as follows

The hard thresholding operator is defined as

$$\begin{aligned} D(U; \lambda) &= U \text{ for all } \text{abs}(U) > \lambda, \\ &= 0 \text{ otherwise} \end{aligned}$$

The soft thresholding operator on the other hand is defined as

$$D(U; \lambda) = \text{sgn}(U) \max(0, |\text{abs}(U)| - \lambda)$$

3.4.3 Threshold determination

The noisy image is represented as a two-dimensional matrix $\{x_{ij}\}$ $i, j = 1 \dots N$. The noisy version of the image is represented as

$$y_{ij} = x_{ij} + n_{ij} \quad i, j = 1 \dots N$$

where n_{ij} are iid as $N(0, \sigma^2)$. We can use the same principles of thresholding and shrinkage to achieve denoising as in 1-D signals.

VisuShrink

Visushrink is thresholding by applying the Universal threshold proposed by Donoho and Johnstone [1]. This threshold is given by

$$\lambda = \sigma * (2 * \log(M))^{1/2}$$

where σ is the noise variance and M is the number of pixels in the image. It is proved in [1] that the maximum of any M values iid as $N(0, \sigma^2)$ will be smaller than the universal threshold with high probability, with the probability approaching 1 as M increases.

SureShrink

Let $\mu = \mu_i$ ($i = 1 \dots d$) be a length d vector, and let $x = x_i$ (with x_i distributed as $N(\mu_i, 1)$) be multivariate normal observations with mean vector μ . Let $b^1 = b^1(x)$ be a fixed estimate of μ based on the observations x . SURE (Stein's unbiased Risk Estimator) is a method for estimating the loss norm($b^1 - \mu$) in an unbiased fashion.

In our case b^1 is the soft threshold estimator $b^1(t)(x) = \Pi(x_i)$. We apply Stein's result to get an unbiased estimate of the risk :

$$\text{SURE}(t; x) = d - 2\# \{i : \text{abs}(x_i) < t\} + \sum (\min(\text{abs}(x_i), t))^2$$

For an observed vector x (in our problem, x is the set of noisy wavelet coefficients in a subband), we want to find the threshold t that minimize SURE($t; x$), i.e

$$t = \text{argmin} \text{SURE}(t; x)$$

The above optimization problem is computationally straightforward.

BayeShrink

We determine the threshold for each subband assuming a Generalized Gaussian Distribution (GGD). The GGD parameters, σ_x need to be estimated to compute the thresholds.

$$\hat{\sigma} = \frac{Median(|Y_{ij}|)}{0.6745}, \quad Y_{ij} \in subbandHH_1$$

$$\hat{\sigma}_Y^2 = \frac{1}{n} \sum_{i,j=1}^n Y_{ij}^2$$

$$\hat{\sigma}_X = \sqrt{\max(\hat{\sigma}_Y^2 - \hat{\sigma}^2, 0)}$$

The above equations were implemented in Matlab. The PSNR for each method was calculated with respect to the wavelet used. Also the images were run through Melanie to obtain the number of spots detected.

3.4.3 Total Variations

While removing noise from image or data, the challenge is to preserve and enhance important features.

Wavelet based thresholding techniques commonly used for de-noising are not good in conserving the directional features. Total variation Method can be used with wavelets results in not only better conservation of directional features but better PSNR performance too.

Total Variation is used with wavelets in following ways :

TV method 1: Use Wavelets Thresholding to reduce the noise first, then Total Variation to further denoise the data or image.

TV method 2: First obtain a denoised image using Wavelet Thresholding. From noisy image subtract the denoised image so that we get the difference image.

Finally TV is applied to de-noise the difference image for extracting the missing details and obtain the detail image, the fusion image of the first denoised image and the final detail image, is the result.

Total Variation Method for de-noising:

Let $u^0(x)$ be original signal which contains clean signal $u(x)$ and noise $n(x)$.

$$u^0(x) = u(x) + n(x)$$

Consider a node say α with neighbors β, γ, δ and τ .

First find out the local variation at each node say α .

$$|\nabla_\alpha u| = \sqrt{\sum_{\beta \sim \alpha} (u_\beta - u_\alpha)^2}$$

For a given noisy signal u^0 , the digital TV filter $F^{l,a}$ is a nonlinear data-dependent filter

$$F^{l,a} : u \rightarrow v$$

For any node α we apply TV filter by

$$v_\alpha = F_\alpha(u) = \sum_{\beta \sim \alpha} h_{\alpha\beta}(u) u_\beta + h_{\alpha\alpha}(u) * u^0_\alpha.$$

Here filter coefficients are given by

$$h_{\alpha\beta}(u) = \frac{w_{\alpha\beta}}{(\lambda + \sum_{\gamma \sim \alpha} w_{\alpha\gamma})}, \quad h_{\alpha\alpha}(u) = \frac{\lambda}{(\lambda + \sum_{\gamma \sim \alpha} w_{\alpha\gamma})}$$

$$w_{\alpha\beta}(u) = \frac{1}{|\nabla_\alpha u|_a} + \frac{1}{|\nabla_\beta u|_a}$$

$$|\nabla_\alpha u|_a = \sqrt{(|\nabla_\alpha u|^2 + a^2)}$$

Where

The complete algorithm at node is therefore as follows.

1) TV Filtering at α :

compute the local variation at and all its neighbors β ;

compute the weights $w_{\alpha,\beta}$.

compute the filter coefficients $h_{\alpha\beta}, h_{\alpha\alpha}$

filtering: $F_\alpha(u) = \sum_{\beta \sim \alpha} h_{\alpha\beta} u_\beta + h_{\alpha\alpha} * u^0_\alpha$.

Assign a linear order to all nodes

$\alpha_1 < \alpha_2 < \alpha_3 \dots \dots < \alpha_n$

2) Then the process of TV filtering is defined as follows

Initialize $u^{(0)}$ by setting $u^{(0)} = u^0$, typically not necessarily.

For $k=1,2,3\dots n$

$$u_{\alpha j}^k = F_{\alpha j}^k(u^{k-1})$$

End

End

Parameter ‘ a ’ is set around 0.0001, it is introduced to avoid division by zero. Parameter ‘ λ ’ is important for the restoration effect. An estimation of the optimal λ from current signal is given by :

$$\lambda \simeq \frac{1}{\sigma^2} \frac{1}{|\Omega|} \sum_{\alpha \in \Omega} \sum_{\beta \sim \alpha} w_{\alpha\beta} (u_\beta - u_\alpha)(u_\alpha - u_\alpha^0).$$

3.4.4 Complex wavelet transform

DWT and its disadvantages in image processing

In discrete wavelet transform (DWT) any finite energy signal $x(t)$ can be decomposed in terms of wavelet $\Psi(\cdot)$ and scaling function $\phi(\cdot)$ is given below

$$x(t) = \sum_{n=-\infty}^{\infty} c(n) \phi(t-n) + \sum_{j=0}^{\infty} \sum_{n=-\infty}^{\infty} d(j, n) 2^{j/2} \psi(2^j t - n).$$

(1)

Where

$$\begin{aligned} c(n) &= \int_{-\infty}^{\infty} x(t) \phi(t-n) dt, \\ d(j, n) &= 2^{j/2} \int_{-\infty}^{\infty} x(t) \psi(2^j t - n) dt. \end{aligned} \quad (2)$$

Disadvantages of DWT

1. Oscillations

Since wavelets are band pass functions, the wavelet coefficients tend to oscillate positive and negative around singularities. This considerably complicates wavelet-based processing, making singularity extraction and signal modeling, in particular very challenging. Moreover, since an oscillating function passes often through zero, we see that singularities yield large wavelet coefficients. It is quite possible for a wavelet overlapping a singularity to have a small or even zero wavelet coefficient [22].

2. Aliasing

The wide spacing of the wavelet coefficient samples, or equivalently, the fact that the wavelet coefficients are computed via iterated discrete time down sampling operations interspersed with non-ideal low pass and high pass filters, results in substantial aliasing. The inverse DWT cancels this aliasing, of course, but only if the wavelet and scaling coefficients are not changed. Any wavelet coefficient processing (thresholding, filtering, and quantization) upsets the delicate balance between the forward and inverse transforms, leading to artifacts in the reconstructed signal [22].

3. Shift variance

A small shift of the signal greatly perturbs the wavelet coefficient oscillation pattern around singularities. Shift variance also complicates wavelet-domain processing algorithms must be made capable of coping with the wide range of possible wavelet coefficient patterns caused by shifted singularities [22].

4. Lack of directionality

Finally, while Fourier sinusoids in higher dimensions correspond to highly directional plane waves, the standard tensor product construction of M-D wavelets produces a checkerboard pattern that is simultaneously oriented along several directions. This lack of directional selectivity greatly complicates modeling and processing of geometric image features like ridges and edges [22].

Dual tree complex wavelet transforms

Dual tree CWT employs two real DWTs where the first DWT gives the real part of the transform while the second DWT gives the imaginary part. The analysis and synthesis FBs used to implement the dual-tree CWT and its inverse is illustrated in figures (3) and (4). The two real wavelet transforms use two different sets of filters, with each satisfying the PR conditions. The two sets of filters are jointly designed so that the overall transform is approximately analytic. Let $h_0(n)$, $h_1(n)$ denote the low-pass/high-pass filter pair for the upper FB (tree A), and let $g_0(n)$, $g_1(n)$ denote the low-pass/high-pass filter pair for the lower FB (tree B). We will denote the two real wavelets associated with each of the two real wavelet transforms as $\psi_h(t)$ and $\psi_g(t)$. In addition to satisfy the PR conditions, the filters are designed so that the complex wavelet $\psi_c(t) = \psi_h(t) + j\psi_g(t)$ is approximately analytic. Equivalently, they are designed so that $\psi_g(t)$ is approximately the Hilbert transform of $\psi_h(t)$ [denoted $\psi_g(t) \approx H\{\psi_h(t)\}$].

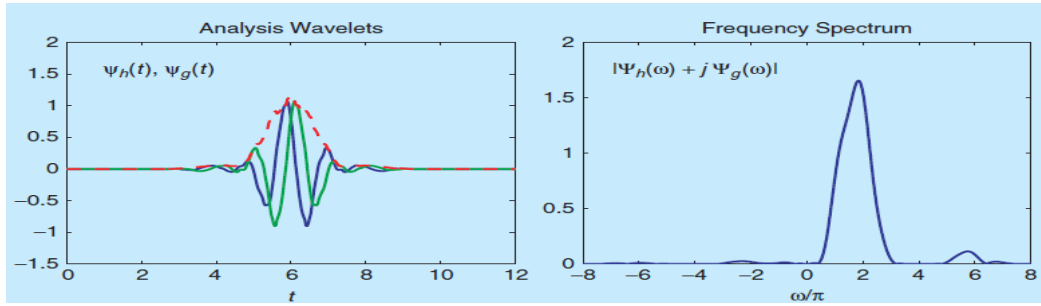


Fig Represents the complex wavelet function in analysis filter and approximately analytic [22].

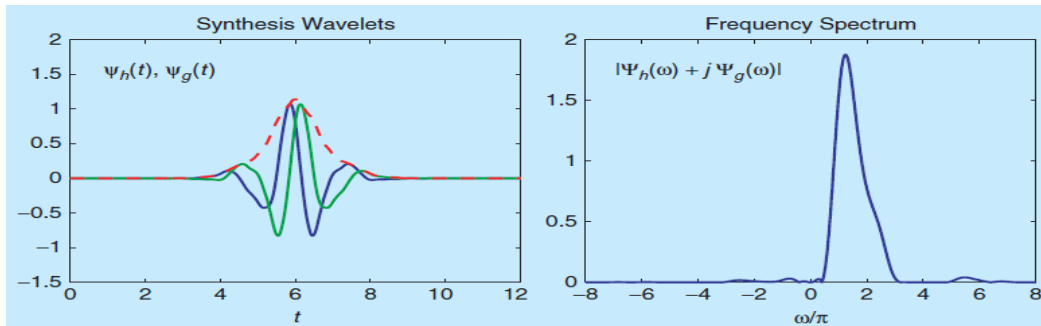


Fig Represents the complex wavelet function in synthesis filter and approximately analytic [22]. Analysis filter bank in dual tree CWT

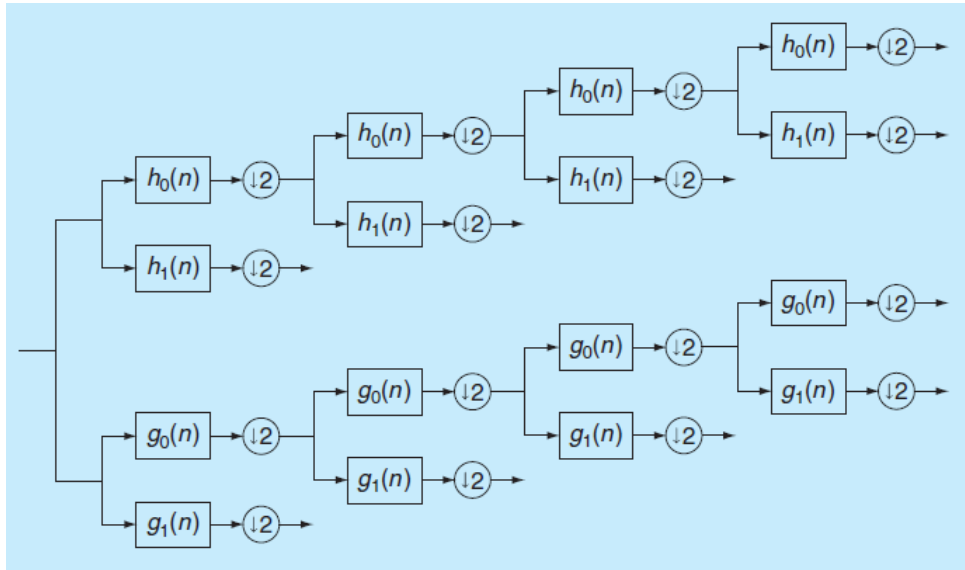


Fig . Analysis filter bank [22]

Synthesis filter bank in CWT

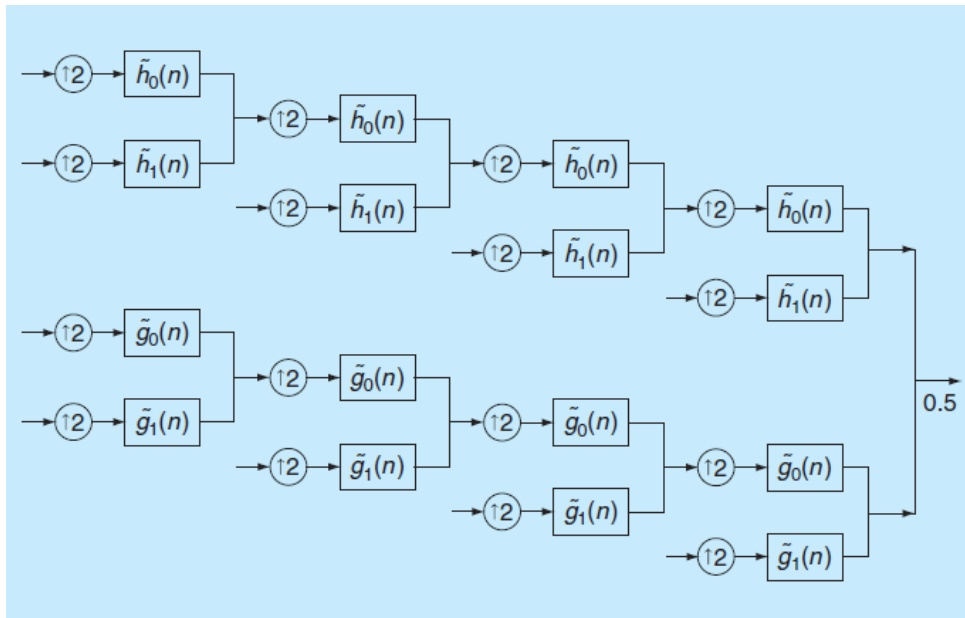


Fig . Synthesis filter bank [22].

The inverse of the dual-tree CWT is as simple as the forward transform. To invert the transform, the real part and the imaginary part are each inverted the inverse of each of the two real DWTs are used to obtain two real signals. These two real signals are then averaged to obtain the final output. Note that the original signal $x(n)$ can be recovered from either the real part or the imaginary part alone.

Half sample delay condition

The design of low pass and high pass filters in branch A and branch B such that corresponding scaling and wavelet function form an approximate Hilbert transform pair ie, $\Psi g(t) \approx H\{\Psi h(t)\}$, $\phi g(t) \approx H\{\phi h(t)\}$. where

$$\psi_h(t) = \sqrt{2} \sum_n h_1(n) \phi_h(t),$$

$$\phi_h(t) = \sqrt{2} \sum_n h_0(n) \phi_h(t),$$

So the low pass filter response of branch B given by $g_0(n) \approx h_0(n - 0.5)$ [23]. That will result in $\psi g(t) \approx H\{\psi h(t)\}$. Since the filter coefficients are defined in integers, this given half sample delay is informal [23].

Implementation of dual tree CWT

As shown in figure 3 the low/high pass filters of branch A and B are designed. Respective coefficients of low/high pass filters for branch A denoted by H_{0a} and H_{0b} and for branch B H_{0b} and H_{1b} in table 1. Here we have done first level decomposition for branch A, B and from the resultant sub band coefficients found out the complex coefficients ($LL_a + i^*LL_b$). Image denoising procedures are done on these complex coefficients. The filter coefficients are calculated based on q shift method, $g_0(n) = h_0(N - 1 - n)$. Where $g_0(n)$ and $h_0(n)$ are the low pass filter coefficients of branch B and A. That is, $h_0(n)$ is an approximately linear-phase filter and is symmetric around the point $n = 0.5(N - 1) - 0.25$ [22].

H_{0a}	H_{1a}	H_{0b}	H_{1b}
0	0	0.01122679	0
-0.08838834	-0.01122679	0.01122679	0
0.08838834	0.01122679	-0.08838834	-0.08838834
0.69587998	0.08838834	0.08838834	-0.08838834
0.69587998	0.08838834	0.69587998	0.69587998
0.08838834	-0.69587998	0.69587998	-0.69587998
-0.08838834	0.69587998	0.08838834	0.08838834
0.01122679	-0.08838834	-0.08838834	0.08838834
0.01122679	-0.08838834	0	0.01122679
0	0	0	-0.01122679

Table 1. The filter coefficients for 1st stage decomposition H_{0a} , H_{1a} represents low/high pass of tree A H_{0b} , H_{1b} represents low/high pass of tree B.

Denoising

The CWT can give a substantial performance boost to DWT noise reduction algorithms. When thresholding the complex-valued coefficients of the CWT it is typically more effective to apply the nonlinearity to the magnitude rather than to the real and imaginary parts separately. Since the coefficient magnitudes are slowly varying and free of aliasing distortion, this results in a nearly shift invariant denoising algorithm. Also, denoising algorithms based on statistical models of wavelet coefficients can be more effective for the CWT than for the real DWT because the magnitudes of the coefficients are more strongly dependent in inter-scale and intra-scale neighborhoods.

3.4.5 Results

Spots according to mpiib-berlin.mpg.de database = 632

Without TV

Technique	Hard Visu	Hard Sure	Hard Bayes	Soft Visu	Soft Sure	Soft Bayes
Wavelet Used						
Daub2	11.6886	13.8115	13.8299	11.488	13.8166	13.8272
Daub4	17.7331	17.7467	17.7808	17.7331	17.756	17.8323
Daub6	16.4356	16.9876	17.0751	17.8998	18.0289	18.5647
Coif6	17.9854	18.3478	18.9823	18.0293	18.5648	19.5642
Spots Detected	472	477	476	476	480	488

TV method 1

Technique	Hard Visu	Hard Sure	Hard Bayes	Soft Visu	Soft Sure	Soft Bayes
Wavelet Used						
Daub2	20.6731	23.5043	24.4437	20.537	24.5043	24.7716
Daub4	24.4976	24.5576	24.5944	24.6602	24.6809	24.777
Daub6	24.5642	24.7659	25.6421	25.7865	26.2332	27.181
Coif6	25.346	24.8973	25.5768	26.2841	27.8750	28.0912
Spots Detected	434	449	451	451	453	462

TV method 2

Technique	Hard Visu	Hard Sure	Hard Bayes	Soft Visu	Soft Sure	Soft Bayes
Wavelet Used						
Daub2	37.8078	49.6697	59.1047	37.8078	49.5952	54.7561
Daub4	38.9807	51.022	59.9865	39.4567	52.5647	57.873
Daub6	45.5610	53.4839	54.7623	46.2378	54.1039	57.9834
Coif6	49.0988	53.5641	55.8762	52.8734	55.9823	58.3418
Spots detected	492	492	492	495	498	498

Complex Wavelet Transform:

Technique	Hard Visu	Hard Sure	Hard Bayes	Soft Visu	Soft Sure	Soft Bayes
PSNR Values	55.6983	56.4820	56.8291	57.489	58.3904	59.4839
Spots detected	522	539	539	539	539	540

3.5 Introduction to Segmentation

Although this technique is powerful, mature, and sensitive, questions remain concerning its ability to characterize all of the elements of a proteome. 2DGE images are gradient images which have high pixel values at object edges and low pixel values elsewhere. Analysing 2DGE images is quite challenging because of the presence of non-linear background, which depends on the composition of gel; horizontal and vertical streaks and different kinds of irregular spots, viz., overlapped spots due to inadequate separation of proteins, faint spots due to improper detection of spots, spurious spots or fake spots due to probable contamination and saturated spots due to improper staining. All these challenges reduce the accuracy in proper segmentation of protein spots.

A variety of different methodologies have been proposed in the literature intended to solve the spot-detection or segmentation issue. These include edge detection algorithms such as the Laplacian filtering, in conjunction with smoothing or morphological operators , thresholding methods based on 1D histograms , spot-segmentation techniques based on watershed methods , and statistical spot modelling techniques using Gaussian fitting and diffusion models.

However, all of these methods have some drawbacks which make their implementation not so productive in 2DGE image analysis. Edge detection method does not perform well in low quality images. Thresholding method fails to detect and accurately segment the protein spots since a 1D histogram does not provide information on the spatial correlation between the pixels in the image. Spot segmentation using Watershed method causes over-segmentation. The statistical spot modelling techniques requires the initial assumption that the spots have a specific common shape and size which is not always true.

Consequently, these well-established programs and techniques require human interventions which limit the throughput and bring the objectivity and reproducibility of results into question. Therefore, automating this part of the process is

essential because: (i) it will allow rapid high-throughput analysis of the expression levels of thousands of proteins, and (ii) it will prevent variations in the protein expression profiles due to subjectivity.

In this paper we'll introduce a novel approach to efficiently detect and segment protein spots on a 2DGE image. The sequence of operations performed in developing our algorithm has never been published to our best knowledge. Our algorithm includes multilevel wavelet decomposition of 2DGE image, application of modified watershed transform on the low resolution image followed by region merging. Region merging, performed on the label matrix obtained from watershed transform, minimizes the intrinsic drawbacks of watershed method, such as over-segmentation and inaccurate watershed lines.

3.5.1 Decomposition using Stationary Wavelet Transform (SWT)

To minimize the over-segmentation issue of watershed transform and optimize the accuracy of segmented image we have used decomposition of the primary 2DGE image using stationary wavelet transform (SWT). The use of SWT makes it easy to reconstruct the original image.

The rational for selecting the above wavelet classes was driven by the normal or Gaussian like characteristics of the wavelets themselves. Since the electrophoretic migration models within the 2DE image in general closely approximate bivariate normal distributions themselves, a wavelet class that too exhibits the same characteristics will adapt and provide better correlation during the transform resulting in better, overall, spot segmentation performance.

3.5.2 Watershed Transform

The Watershed transform is a robust method of image segmentation generally applied on the morphological gradient of the target image. It produces watershed lines at the points of grey value discontinuity. It is a region-growing algorithm

that analyses the image as a topographical surface. The image surface is interpreted as collection of valleys or catchment basins having lower intensity and separated by watershed lines or ‘ridges’ having higher intensity pixel values. Before applying watershed method, the input image is converted into its binary form followed by the distance transform which results in the morphological grayscale image of the original input image. Distance transform calculates the Euclidean distances from every pixel to its nearest nonzero-valued pixel.

Transformation of the binary image matrix $A_{M,N}$ is computed as Euclidean distance of each pixel $a_{i,j}$ to the nearest pixel $a_{k,l}$ with the value 1. Resulting matrix $B_{M,N}$ is then formed by elements [5]

$$b_{i,j} = \begin{cases} 0 & \text{for } a_{i,j} = 1 \\ \min_{\forall k,l, a_{k,l}=1} (\sqrt{(i-k)^2 + (j-l)^2}) & \text{for } a_{i,j} = 0 \end{cases}$$

for $i = 1, 2, \dots, M, j = 1, 2, \dots, N$.

1	1	0	0	0
1	1	0	0	0
0	0	0	0	0
0	0	0	0	0
0	1	1	1	0

0.00	0.00	1.00	2.00	3.00
0.00	0.00	1.00	2.00	3.00
1.00	1.00	1.41	2.00	2.24
1.41	1.00	1.00	1.00	1.41
1.00	0.00	0.00	0.00	1.00

A small binary image (left) and its distance transform (right).

The watershed transform gives a label matrix which contains 0’s and region indices (1, 2, 3... etc.). This label matrix is further used to identify the watershed regions with its integer elements. Its zero values identify image contours or watershed lines and nonzero elements belong to watershed regions or catchment basins.

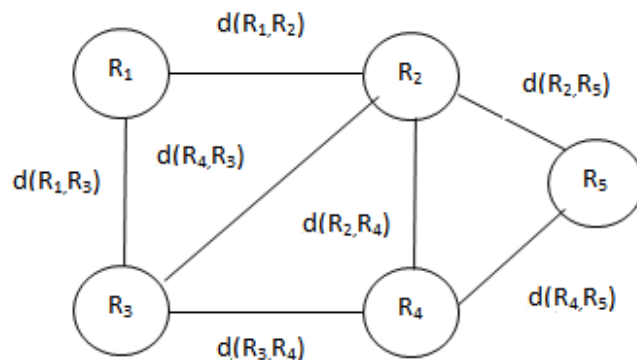
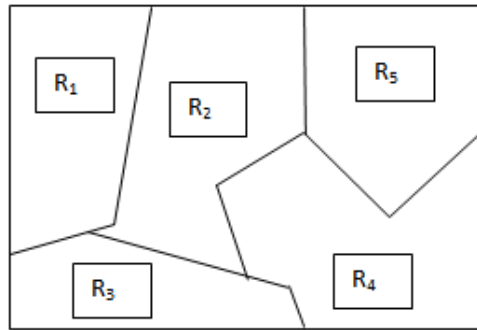
The key idea of watershed transform is to change the starting image into another one whose catchment basins are the objects or regions that we want to identify.

Advantage of this algorithm is that it produces closed, adjacent and accurate contours. Since a low-pass filter is involved, noise suppression is inherent to this transform [6]. The major drawback of watershed method is oversegmentation of image which occurs because every regional minimum, even if tiny and insignificant, forms its own catchment basin. The presence of non-

linearity and noise in the image also increase over-segmentation. To minimize this problem decomposition of image using stationary wavelet transform (SWT) have been performed which resulted in a low resolution image. The morphological counterpart of this image confers improved results when operated with watershed method. Further improvement in the quality and accuracy of the segmented image were achieved by region merging. In this method, the immediate neighbours of every protein spots were detected and they were de-differentiated or merged according to the difference of their respective moment values (sum of mean, variance and skewness), based on a specific pre-defined threshold values.

3.5.3 Region Merging

The region merging process is formulated as a graph-based clustering problem. A graph G is used to represent the information upon which the region merging process is based. In the following figure, each node in G represents one of the segmented regions in the set $I = \{R_1, R_2, \dots, R_k\}$.



Each edge of G corresponds to a sum of the moment values (mv), which can be used to compare the mv of adjacent regions. Our decision on which regions to merge is determined through homogeneity and similarity criteria based on the

wavelet coefficients. Each of the segmented regions will have mean, second- and third-order central moment values of the wavelet coefficients calculated. For each region R_i of the segmented image, we calculate the mean (M), second- (μ_2) and third-order (μ_3) central moments of the region as,

$$M = \frac{1}{\text{num}(R_i)} \sum \sum R_i(x, y) \quad \forall x, y \in R_i$$

$$\mu_2 = \frac{1}{\text{num}(R_i)} \sum \sum (R_i(x, y) - M)^2$$

$$\mu_3 = \frac{1}{\text{num}(R_i)} \sum \sum (R_i(x, y) - M)^3$$

where $\text{num}(R_i)$ is the number of pixels of segmented region i .

To merge the segmented regions using similarity criteria (d), we can use the following equation:

$$\text{mv}_i = \frac{1}{N} (R(M_i) + R(\mu_{2i}) + R(\mu_{3i}))$$

$$i = 1, \dots, N$$

$$d(R_i, R_j) = (\text{mv}_i - \text{mv}_j)^2$$

$$\forall i, j \in \{1, \dots, N, \text{ for } i \neq j\}$$

where mv_i is the similarity value of segmented region i and N is the number of segmented regions. $R(M)$, $R(\mu_2)$ and $R(\mu_3)$ are the mean, second- and third-order moment values of the segmented region, respectively. If the mv values of the adjacent regions satisfy a specified value, two adjacent regions. The specified values are found by experimentation.

3.5.4 Results

The original image was segmented using watershed transform along with distance transform. A significant amount of oversegmentation was observed. To reduce this oversegmentation, various wavelets:

- Haar
- Daub 4

- Daub 6
- Daub 8

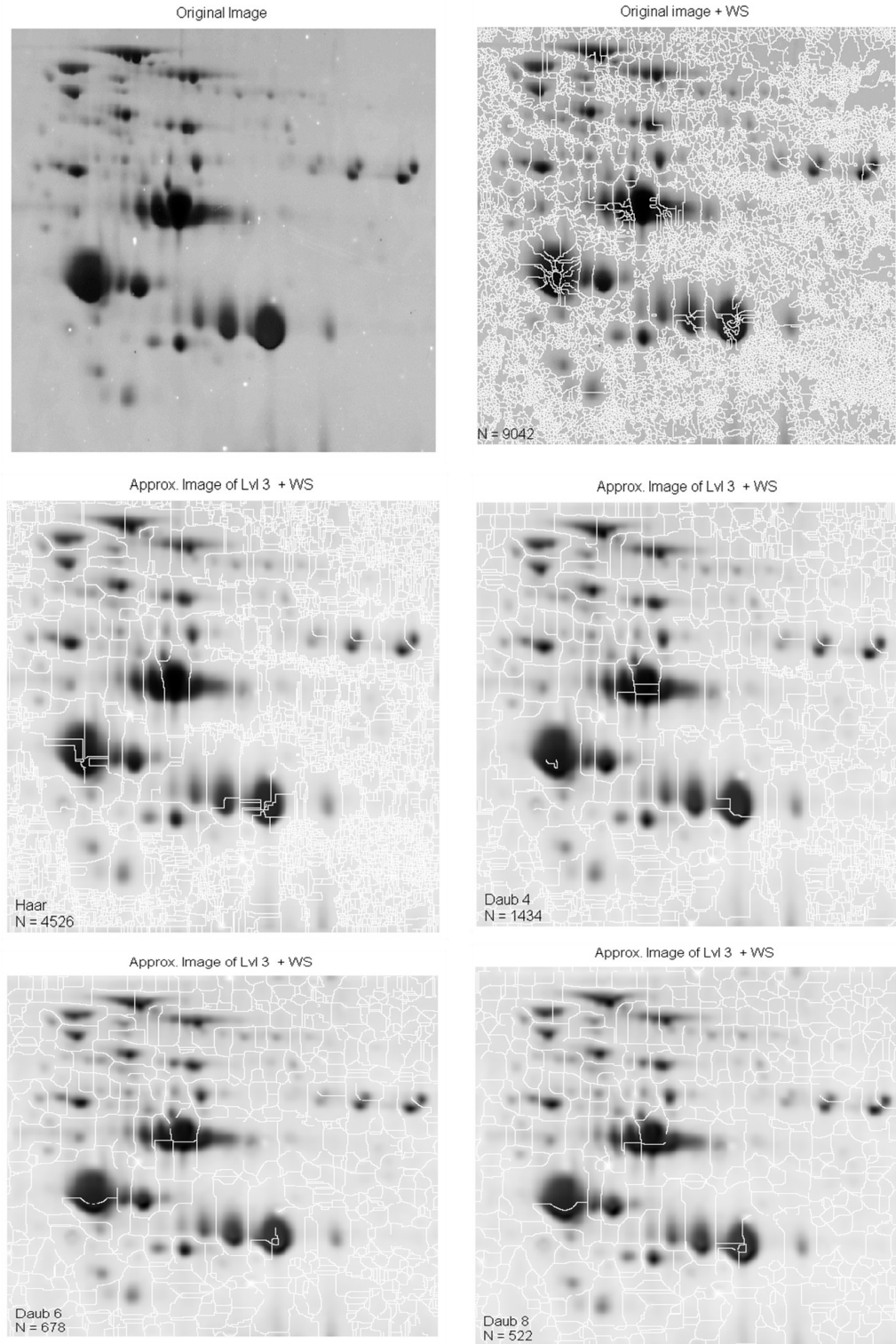
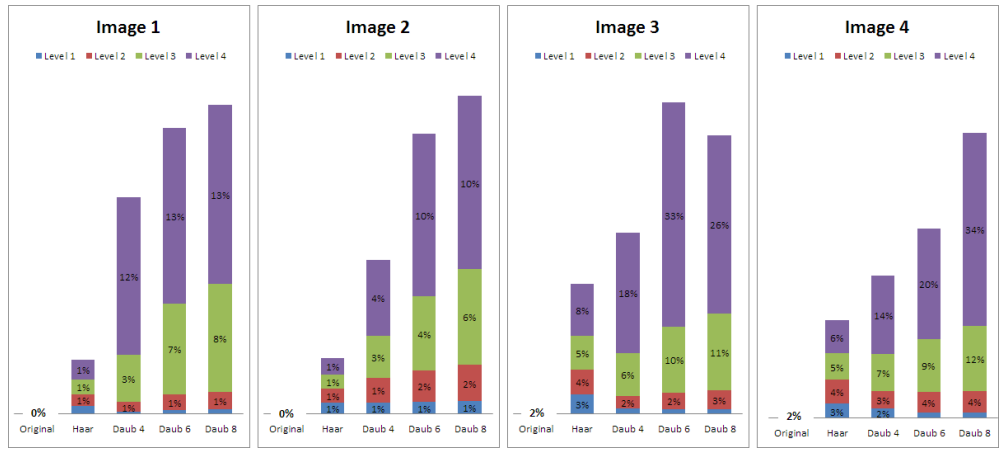
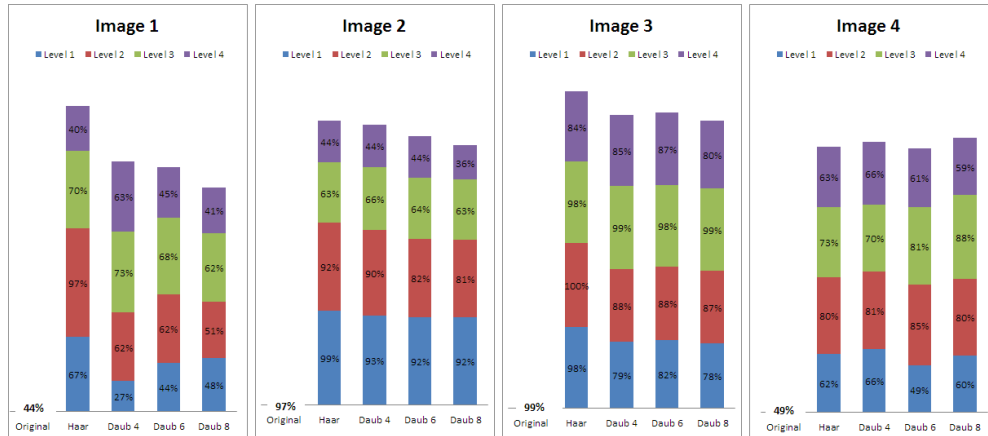


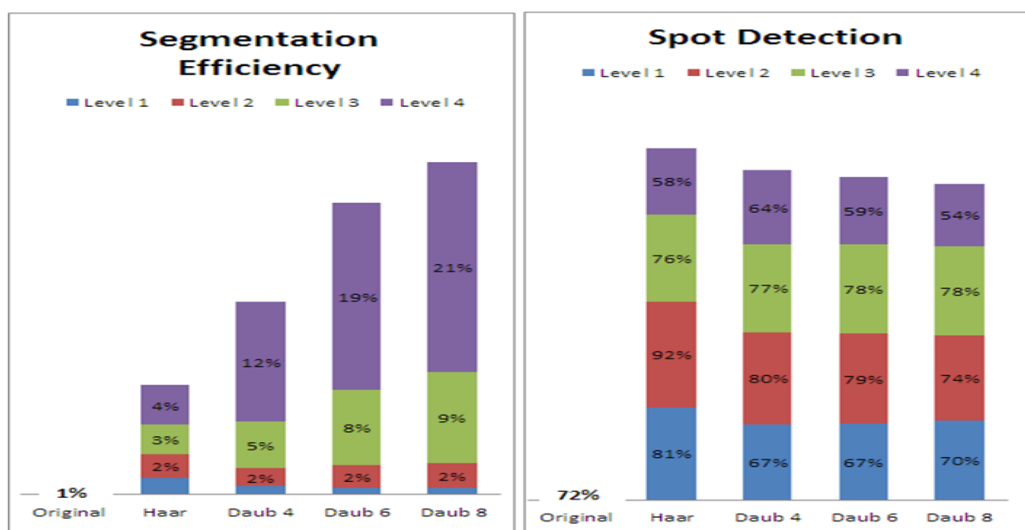
Fig : Segmented Images



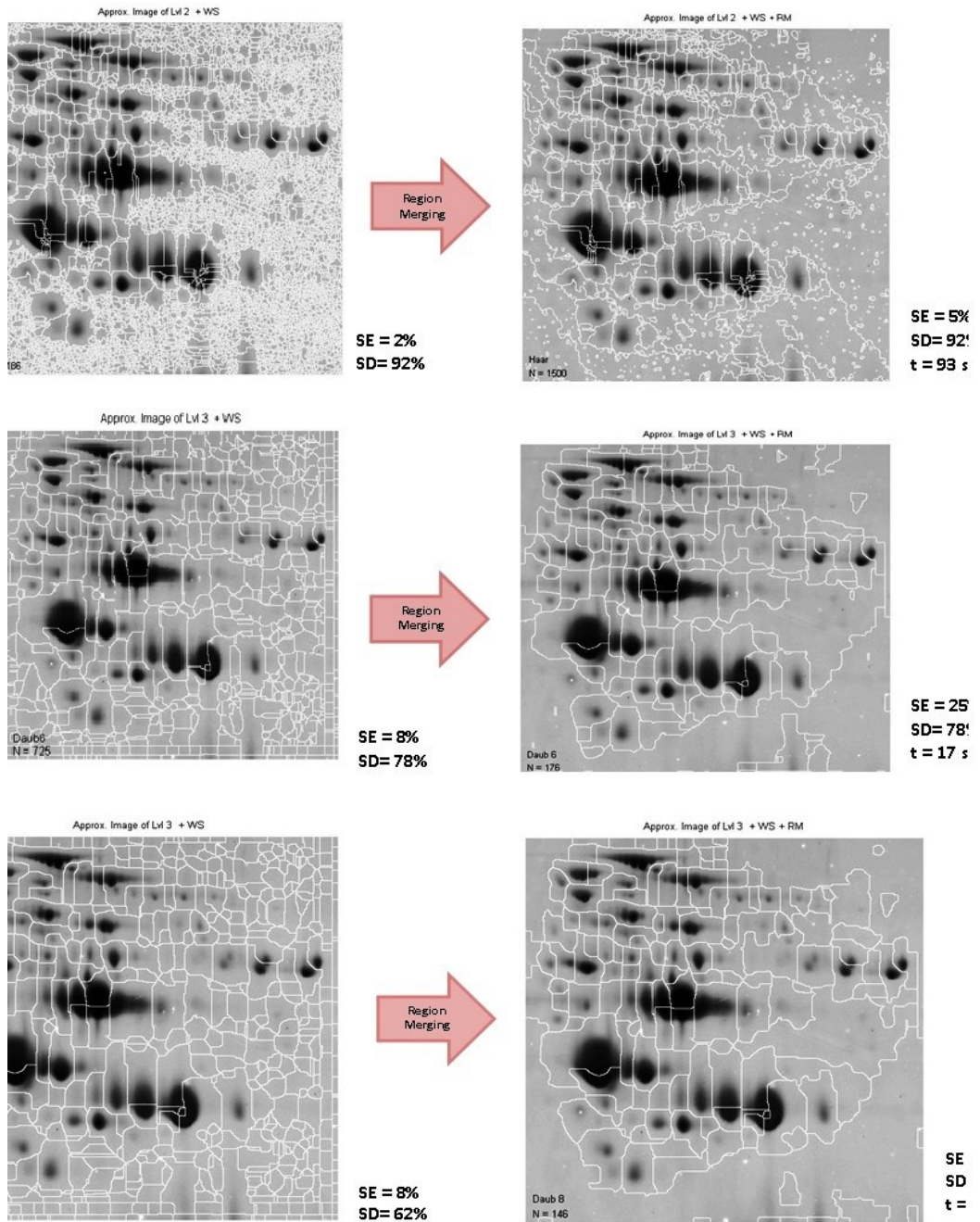
The above graphs compile the segmentation efficiency of the four images shown in the previous tables.



The above graphs compile the spot detection in the four images shown in the previous tables.



The above graphs give the average segmentation efficiency and spot detection for the four images



CHAPTER 4

Summary, Discussion and Conclusion

4 Summary, Discussion and Conclusion

4.1 Comparative study of wavelets

From the Results, it can be observed that for unihard thresholding, the performance of all wavelets is similar except for Haar. For unisoft only coiflet and daubechies show a satisfactory performance. But excellent results are obtained for Bayes thresholding. While the performance for coiflet and daubechies is almost constant, quincunx and undecimated quincunx provide some very good results in almost all cases. Therefore, we conclude that **Best denoising can be achieved by Bayes soft thresholding using quincunx or undecimated quincunx transforms.**

From results we can clearly see that this parameter is best manifested by the coiflet wavelet of order 1 and worst by daubechies of order 15. Strangely, we have observed that the performance of wavelets of the same family worsens as we raise the order of the wavelets. We conclude that coiflet of order 1 provides the best characterization of true spots.

Other attempts at finding parameters: We also tried various other parameters and methods to differentiate true and fake spots without much success. Some of our attempts are mentioned here:

We tried taking pixel-wise product of sub-bands of same level transform thinking that the singularities will be enhanced and randomness will be reduced. This method does not work, as get very low intensity values in the resultant image.

We also took pixel-wise product of sub-bands of different levels transforms. This method does not help in identifying true protein spots.

We removed smallest 10% coefficient from the detailed bands and reconstructed the image in order to find out in which case, maximum information about singularities is stored in minimum number of pixels. We could not propose a good measure to compare the results.

Limitations

For comparison of denoising achieved by each wavelet, we have first added gaussian noise on original image and then denoised the noisy image. Therefore, the results we get using this method may not hold in cases where noise is not gaussian, especially when the noise is multiplicative. But since we have no other parameter to quantify noise in an image, we have compared the performance only using psnr values.

4.2 Image De-Noising, using statistical model

We tested the algorithm on a number of images and report results for all *sets of different gel images*. We have an orthogonal wavelet transform with five levels of decomposition and Daubechies' length-8 wavelet. Centered square-shaped windows of sizes 3×3 , 5×5 and 7×7 were employed to find different estimates for $\sigma^2(k)$. The parameter λ of the prior $f\sigma$ was set equal to the inverse of the standard deviation of wavelet coefficients that were initially denoised by using and linear MMSE-like estimation.

We compared five different denoising methods. The PSNR results are shown in bar graph in previous section. The first method is the hard-thresholding of wavelet coefficients using a constant threshold for all subbands, calculated. The second method is MATLAB's image denoising algorithm *wiener2*. The third method uses spatially adaptive wavelet thresholding. We included only the results from which were obtained by using an orthogonal wavelet transform since this is equivalent to our setup.

Our results are presented for two different methods. First, we treated the vari-

ances as deterministic quantities and computed approximate ML estimates. We call the resulting method **LAWML** (Locally Adaptive Window-based denoising using ML). The second method uses an exponential distribution as a prior for the underlying variance field. Based on this model, we compute approximate MAP estimates of the variances. This method is called as**LAW-MAP** (Locally Adaptive Window-based denoising using MAP).

In this work, we confined ourselves to square-shaped neighborhoods with fixed size, for simplicity. In general, it would be desirable to automatically select both the size and the shape of the neighborhood region. But clearly, this would introduce additional difficulties. The selection of the window size suggests a trade-off which has been discussed in detail in. The flexibility of method lends itself to the usage of different shaped neighborhoods for each coefficient. This could be implemented by using edge- and shape-adapted windows. Such an adaptation is likely to further improve denoising performance, see for an example.

4.3 Image De-Noising, non-parametric approach

From the obtained data (please refer previous section) we concluded that complex wavelet transform which provides extra directional information shines on all three parameters. It has high PSNR values, Visually appealing images were produced and spots detected also were high. The TV filter did provide better results as far as image quality and spots were concerned. Coiflet wavelet was better among the rest of the wavelets used. Also Bayes thresholding coupled with soft thresholding worked well.

4.4 Image Segmentation

It was noted as the length of the filter increased the number of segmented region (N) decreased. As the length of filter increased, the identification of overlapped spots was compromised.

CHAPTER 5

REFERENCES

- [1]Generalized Coiflets: A New Family of Orthonormal Wavelets (1997)' by Dong Wei , Alan C. Bovik , Brian L. Evans
- [2]Effective Denoising of 2D Gel Proteomics Images using Contourlets by Tsakanikas P
- [3] M. K. Mih,cak, I. Kozintsev, and K. Ramchandran, "Spatially adaptive statistical modeling of wavelet image coefficients and its application to denoising," in Proc. IEEE Int. Conf. Acoust., Speech, and Signal Proc., vol. 6, Phoenix, AZ, pp. 3253–3256, March 1999.
- [4]Iain M.Johnstone David L Donoho. Adapting to smoothness via wavelet shrinkage. *Journal of the Statistical Association* , 90(432):1200–1224, Dec 1995.
- [5]David L Donoho. Ideal spatial adaptation by wavelet shrinkage. *Biometrika* , 81(3):425–455,August 1994.
- [6]David L Donoho. De-noising by soft threshold-ing. *IEEE Transactions on Information Theory* ,41(3):613–627, May 1995.
- [7]Maarten Jansen. Noise Reduction by Wavelet Thresholding , volume 161. Springer Verlag, United States of America, 1 edition, 2001.
- [8]Martin Vetterli S Grace Chang, Bin Yu. Adaptive wavelet thresholding for image denoising and compression. *IEEE Transactions on Image Processing* , 9 (9):1532–1546, Sep 2000.
- [9]Carl Taswell. The what, how and why of wavelet shrinkage denoising. *Computing in Science and Engineering* , pages 12–19, May/June 2000.
- [10]Anderson NL, Anderson NG, "Proteome and proteomics: new technologies, new concepts, and new words", *Electrophoresis* 19 (11): 1853–61, 1998.
- [11]Blackstock WP, Weir MP, "Proteomics: quantitative and physical mapping of cellular proteins", *Trends Biotechnology*, 17 (3): 121–7, 1999.
- [12]Marc R. Wilkins, Christian Pasquali, Ron D. Appel, Keli Ou, Olivier Golaz, et al., "From Proteins to Proteomes: Large Scale Protein Identification by Two-Dimensional Electrophoresis and Amino Acid Analysis". *Nature Biotechnology* 14 (1): 61–65, 1996.
- [13]Dowsey, A. W., High-throughput image analysis for proteomics. PhD Thesis 2005, Department of Computing, Imperial College London.
- [14]Pietrogrande, M. C., Marchetti, N., Dondi, F., Righetti, P. G., "Spot overlapping in two-dimensional polyacrylamide gel electrophoresis separations: a statistical study of complex protein maps", *Electrophoresis*, 2002, 23, 283-291.
- [15]Kaczmarek, K., Walczak, B., de Jong, S., Vandeginste, B. G. M., Preprocessing of two-dimensional gel electrophoresis images. *Proteomics* 2004, 4, 2377-2389.
- [16]Appel, R. D., Vargas, J. R., Palagi, P. M., Walther, D., et al., "Melanie II – a third-generation software package for analysis of two-dimensional electrophoresis images: II. Algorithms", *Electrophoresis*, 1997, 18, 2735-2748.
- [17]Tyson, J. J., Haralick, R. H., "Computer analysis of two-dimensional gels by a general image processing system", *Electrophoresis*, 1986, 7, 107-113.
- [18]Sternberg, S. R., "Gray scale morphology", *Comp. Vis. Graph. Image Processing*, 1986, 333-355.

- [19] L.Vincent, "Morphological grayscale reconstruction in image analysis: applications and efficient algorithms," IEEE Trans. on Image Processing, vol. 2, no. 2, pp. 176- 201, 1993.
 - [20] P. Cutler, G. Heald, I.R. White, and J. Ruan, "A novel approach to spot detection for two-dimensional gel electrophoresis images using pixel value collection," Proteomics, vol. 3, pp. 392-401, 2003.
 - [21] Jb.T.M. Roerdink, and A. Meijster, "The Watershed Transform: Definitions, Algorithms and Parallelization Strategies," Fundamenta Informaticae, vol. 41, pp. 187-228, 2001.
 - [22] M Rogers, J Graham and R P Tonge, "Using Statistical Image Models for Objective Evaluation of Spot Detection in 2D Gels", Proteomics, vol 3, pp 879-886, 2003.
 - [24] Ales Prochazka, Oldrich Vysata and Eva Jerhotova, "Wavelet Use for Reduction of Watershed Transform Over-Segmentation in Biomedical Images Processing", IEEE, 2010.
 - [25] Cláudio Rosito Jung, "Combining wavelets and watersheds for robust multiscale image segmentation", Image and Vision Computing 25 (2007) 24–33.
- [26] Brent C. Munsell and Robert J. Barsanti, "Electrophoresis 2D Gel Residual Encoding using Adaptive Wavelets for Image Segmentation", IEEE, 2005